

1. Summary of MA2117 Experiment, ID15, May 2014

Numerous tests involving a range of operating and abuse conditions were performed with the ultimate aim of comparing the behaviour of different cell types and chemistries over various conditions.

Abuse testing of Li-ion batteries can present significant risks to the operator. A test chamber is designed to minimise the risk to operators and beamline equipment during abuse testing (Figure 1.1).

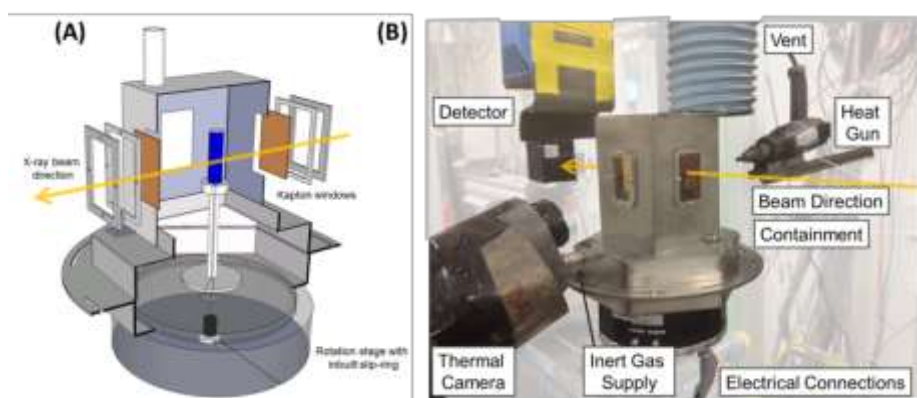


Figure 1.1. Schematic illustration of experimental set-up and 3D reconstructions of test batteries. (A) Cut-away of battery containment design attached to the rotation stage for *in operando* XCT; (B) arrangement of apparatus for XCT battery failure experiments.


Before testing each experiment is assigned a risk level to ensure the operator is aware of the outcome of the test and consider appropriate safety measures. In the following summary of experiments the various tests are assigned to colour coded hazard levels.

Table 1.1. Colour coded hazard levels.

Green	Calm	No venting; no leakage; no fire; no rupture; no explosion, no exothermic reactions or thermal runaway.
Orange	Slightly Aggressive	Leakage; venting; potentially small fire; no explosion; no thermal runaway
Red	Catastrophic	Certain fire; thermal runaway; explosion

An assortment of lithium-ion batteries were tested under extreme thermal and electrical abuse conditions during high frequency X-ray CT at ID15 (Table 1.2).

Table 1.2. Type and properties of batteries tested during high speed *in-operando* tomography.

Type	18650 NMC	18650 A123	CR2 MnO ₂	Turnigy LiPo (LiCo)
Capacity	2.2 Ah	1.1 Ah	Ca. 0.5 Ah	160 mAh
Max V	4.3 V	4 V	3.3 V	3.7 V
Min V	3 V	2 V	2 V	Ca. 2.7
Max I_c	1 C	4 A	None	10 C
Max I_d	1.5 C	30 A	1 A contin.	30 C
				

For ease of reference, the tests are separated by degree of risk, low (Table 2.1), medium (Table 2.2) and high (

Table 2.3). Each of the test conditions is given a label for future reference. Both fast imaging (F) at 0.8 s and 0.4 s per tomogram and slow imaging (S) at 40 s per tomogram was performed.

The most developed results to date are those of two commercial 18650 Li(NMC) batteries (LG 2.2 Ah NMC and LG 2.6 Ah NMC) undergoing thermal runaway which are currently under embargo by Nature Communications as we await publication. Preliminary results for each of the tests are included in the appendices. Appendices include unprocessed tomographs, thermal images and voltage-time plots for each of the abuse tests.

Thermal Abuse involved batteries subjected to high temperatures (ca. 250 °C) using the heat-gun (test label R₁), which was activated when the batteries began to rotate. The continuous rotation helped to maintain a uniform circumferential temperature distribution around the batteries. Heating continued until thermal runaway occurred. The pco dimax camera stored 17 s at 1250 fps. The post-event triggering for recording the images was activated ca. 2 s after the catastrophic outcome of thermal runaway (explosion or violent venting).

Electrical Abuse tests were performed by including an electrical slip-ring to maintain electrical contact with the cell during fast rotations. A potentiostat was connected outside the ID15 hutch to control the current and voltage conditions of the cell.

2. Summary of Experiments

Table 2.1. Low risk experiments with moderate abuse.

Label	Type	Test Details	Repeat	Observations
G ₁	LiPo	60 C (9.6 A) discharge rate from fully charged state. + <i>Post-mortem Scans</i>	2 (S&F)	Temperature reached ca. 200 °C, gas generation with swelling, thermal runaway.
G ₂	CR ₂	Rapid discharge from fully charged state at 8 A (ca. 16 C).	1 (F)	Battery heated to ca. 50 °C. No noticeable change in reconstructions. Battery only discharged by ca. 0.3 V. PTC or other safety device may protect against this.
G ₃	NMC	Overcharge at 6 A to the cut-off voltage (ca. 5.2 V). Slow tomo. + <i>Post-mortem Scans</i>	2 (S)	Voltage and temperature rise to ca. 60 °C followed by circuit breaking and cooling.
G ₄	NMC	Charge from 3 V (discharged state) at 10 A.	1 (S)	Temperature at cap rose rapidly. After about 50 s the current stopped. Experiment was stopped and battery was allowed to cool down before repeating the experiment. Repeated 5 times. PTC limited effect of rapid charge.

Table 2.2. Medium risk experiments.

Label	Type	Test Details	Repeat	Observations
O ₁	NMC	Heat fully charged (4.2 V) to ca. 120 °C (Gun 2 cm away from battery at 400 °C) until venting. + <i>Post-mortem Scans</i>	1 (S)	Battery reached about 160 °C before venting.
O ₂	CR ₂	Heat a fully charged battery to ca. 180. Heat gun set at 480 °C at 2 cm from battery. + <i>Post-mortem Scans</i>	1 (F)	Battery exploded at ca. 180 °C. Sparks and molten material seen extruding from the vent region.
O ₃	CR ₂	Heat a fully charged battery to ca. 180 °C. Heat gun set at 400 °C at 2 cm from battery. + <i>Post-mortem Scans</i>	2 (S)	Battery reached ca. 160 °C before venting and 200 °C before eruption. Metallic liquid seen emerging from the cap.
O ₄	A ₁₂₃	Heat fully charged battery (4.2 V) to 120 °C. Heat gun 2 cm away from battery at 400 °C. + <i>Post-mortem Scans</i>	2 (S)	Vented at 120 °C. Heat gun turned off. Spewing and bubbling continued for ca. 5 mins keeping at ca. 115 °C. Battery cooled down thereafter.
O ₅	LiPo	Overcharge at 3 A until fail. + <i>Post-mortem Scans (Realigned)</i>	3 (S)	Temperature rise, swelling, explosion and fire.
O ₆	LiPo	Heat to 120 °C. Heat gun 2 cm away at 300 °C. + <i>Post-mortem Scans (Realigned)</i>	2 (S)	Temperature rose rapidly. Battery swelled and burst. Artefact in the centre of the image.

O7	CR2	Overcharge the battery at 1 A. + <i>Post-mortem Scans</i>	1 (S)	Temperature reached ca. 80 °C before venting and cooling. After cooling voltage slowly increased over time, possible due to continued lithium diffusion.
O8	CR2	Overcharge the battery at 3 A.	1 (F)	Fast tomo limited experiment to 17 s during which time no significant change was observed in the images.

Table 2.3. High risk experiments.

Label	Type	Test Details	Repeat	Observations
R1	NMC	Heat fully charged battery (4.2 V) to 180 °C. Heat gun set at 480 °C at ca. 1.5 cm from battery. + <i>Post-mortem Scans</i>	3 (1S&2F)	Venting at early stage. Thermal runaway when battery reached about 250 °C after ca. 2 minutes. Thermal runaway and explosion.
R2	NMC	Overcharge at 7A to cut-off limit (ca. 5.3 V) then heat to ca. 180 °C.	1 (S)	Significant heating and current trip when the sample reached ca. 80 °C. Very rapid thermal runaway and catastrophic explosion after 17 s of heating.
R3	A123	Heat fully charged battery (4.2 V) to 180 °C. Heat gun set at 500 °C at ca. 1.5 cm from battery. + <i>Post-mortem Scans</i>	2 (F&S)	Fast tomo: Venting at early stage. Thermal runaway when battery reached about 250 °C after ca. 4 minutes. Venting with liquid spewing soon followed by explosion. Complete ejection of contents. Slow tomo: Heating was different for fast and slow tomos. Constant spinning for fast tomo helped apply the heat uniformly. Slow tomo resulted in heat being focused on one side. The failure for slow tomo did not result in complete ejection.

3.Summary of Results

Green

Test G1

File name: *LiPo_short_6oC_a [slow tomo] & LiPo_short_6oC_act [fast tomo]*

Conditions

LiPo 6o C (9.6 A) discharge rate with fast tomography. Slow and fast tomo scans. Slow tomo did not capture much.

Results

Temperature reached ca. 200 °C, gas generation with swelling, thermal runaway.

Electrical:

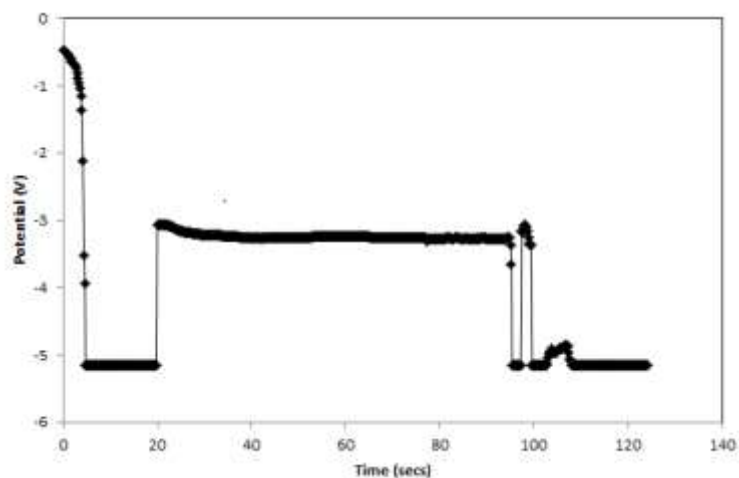


Fig. 1. Cell potential curve during rapid discharge.

Thermal:

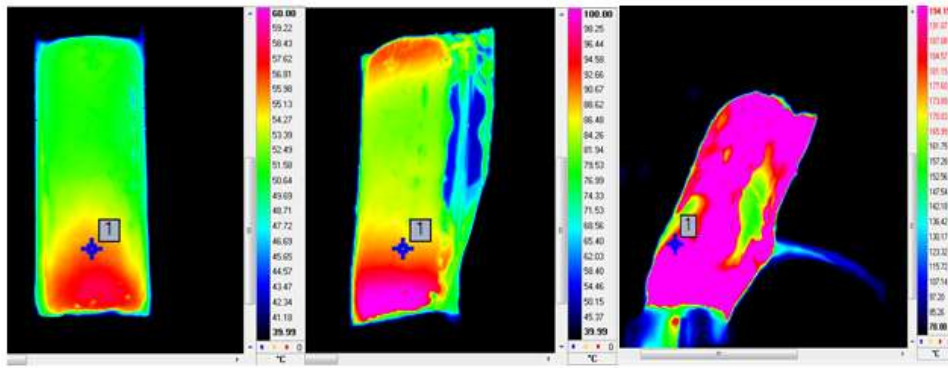


Fig. 2. Thermal image at initial stages of discharge. Thermal image during swelling and before rupture. Thermal image during thermal runaway.

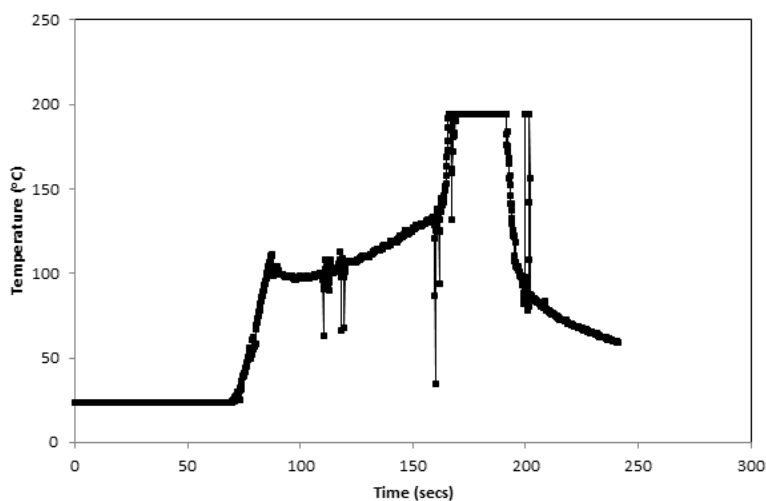


Fig. 3. Temperature reading at point 1 during rapid discharge. The point of rupture and thermal runaway are seen by the two sudden changes in thermal behaviour. The thermal camera was limited to 190 °C for this experiment; hence the peak temperature during thermal runaway was not captured but was >200 °C.

Tomography:

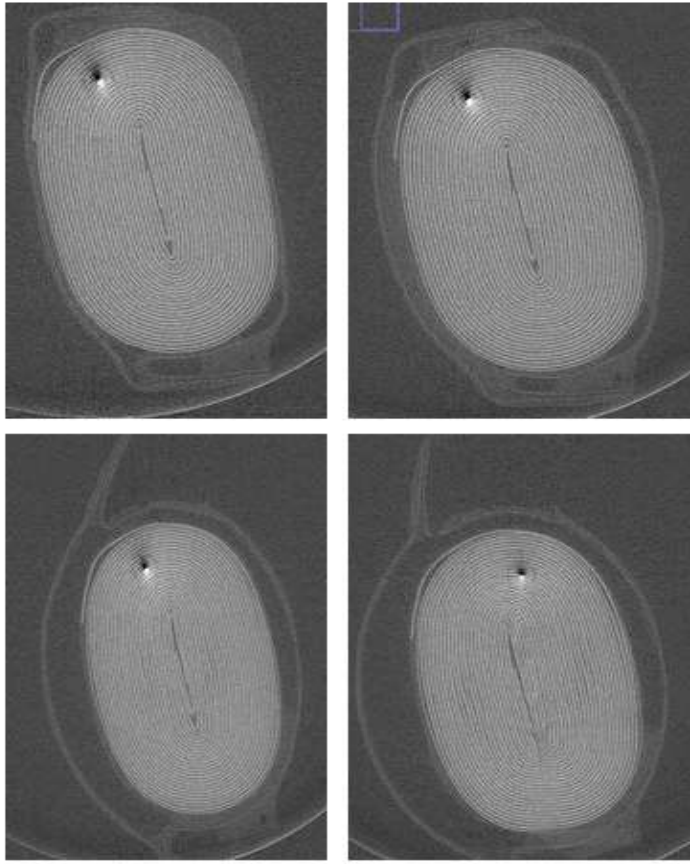


Fig. 4. Sequential tomographs taken over the first 17 s of the rapid discharge abuse test. The initial rapid swelling from internal gas generation is seen.

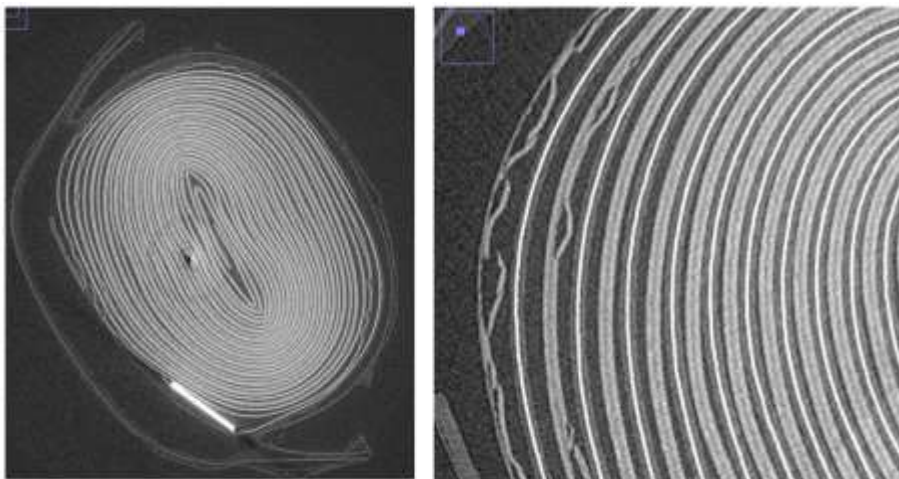


Fig. 5. Postmortem tomograph showing the remnants of the LiPo cell after a rapid discharge abuse test at 60 C (9.6 A). Postmortem tomograph showing delamination of electrode material due to gas evolution.

Comments:

Rapid discharge of the LiPo cells resulted in significant heating causing the batteries to reach $>100\text{ }^{\circ}\text{C}$ before thermal runaway. The gas evolution resulting from the vaporisation of electrolyte material caused the pouch to swell and the electrodes to delaminate.

Test G2

File name: CR2_short

Conditions

CR2 Short-circuit with a 8 A current with fast tomography. Fast tomo captured 17 secs.

Results

Battery heated to ca. $50\text{ }^{\circ}\text{C}$. No noticeable change in reconstructions. Battery only discharged by ca. 0.3 V - PTC or other safety device may protect against this.

Electrical:

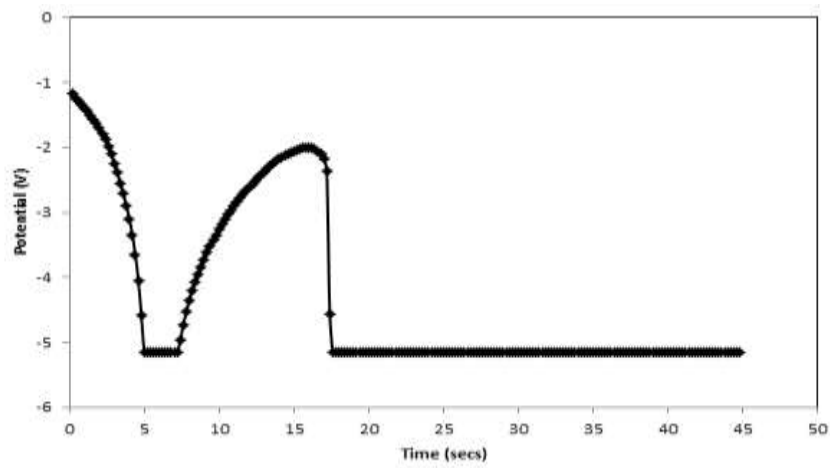


Fig. 6. Potential curve during 8 A rapid discharge of CR2 battery.

Thermal:

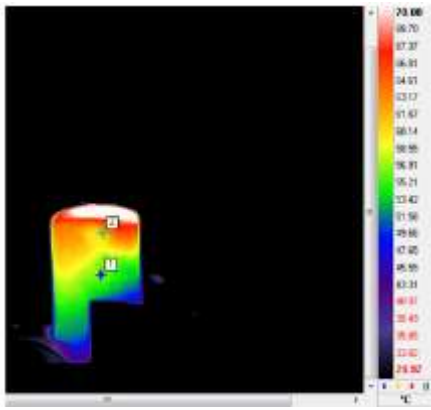


Fig. 7. Thermal image showing temperature gradient across Duracell CR2 battery during rapid (8 A) discharge.

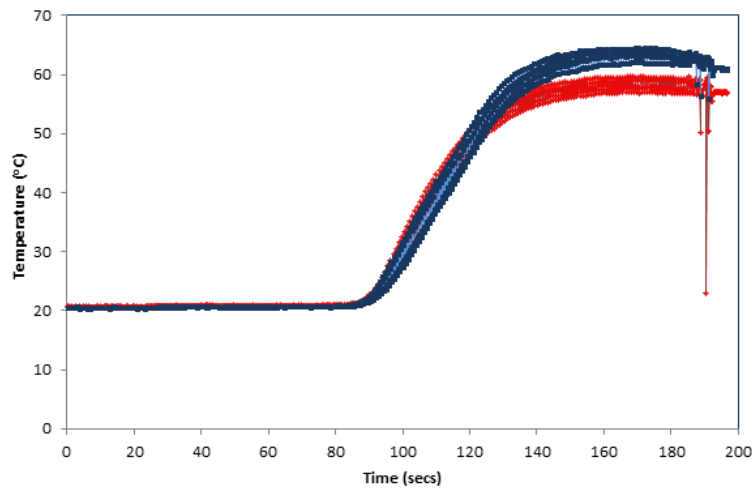


Fig. 8. Temperature reading at point 1 and 2 during 8 A rapid discharge of Duracell CR2 battery.

Tomography:

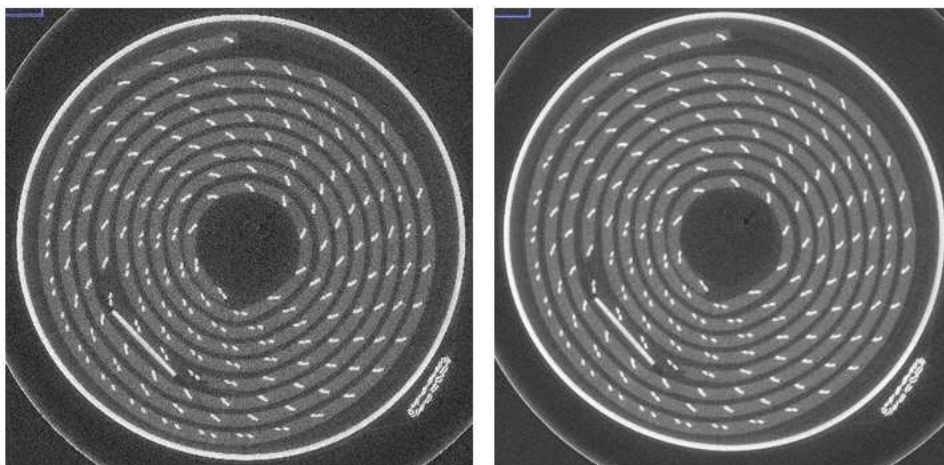


Fig. 9. Tomograph of CR2 battery at the beginning of 8 A rapid discharge. Tomograph of CR2 battery after 17 s of 8 A rapid discharge began.

Comments:

Over 17 s of 8 A discharge there was no noticeable change in the electrode structure and no visible evidence of degradation. The increasing potential over the first 5 s indicates an increase in resistance potentially caused by the PTC. This would have limited the current flowing through the device. The region of the PTC in the thermal images appears to get significantly hotter than the main body of the battery which also indicates the activity of the PTC.

Test G₃

File name: NMC22Overcharge6A_a [& b]

Conditions

2.2 Ah NMC Overcharge at 6 A to the cut-off voltage (ca. 5.2 V). Slow tomo.

Results

Voltage and temperature rise to ca. 60 °C followed by circuit breaking and cooling. Apparent gas pocket between the electrode and separator layers.

Electrical:

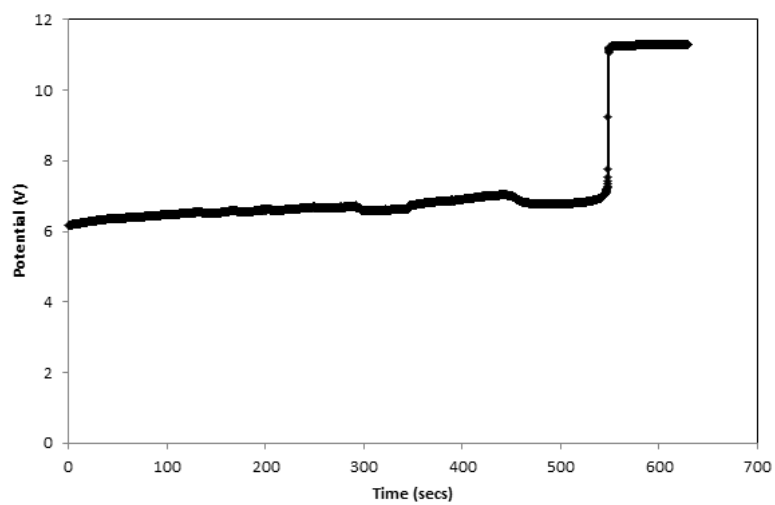


Fig. 10. Battery potential during galvanostatic overcharging at 6A of an 18650 2.2 Ah NMC battery.

Thermal:

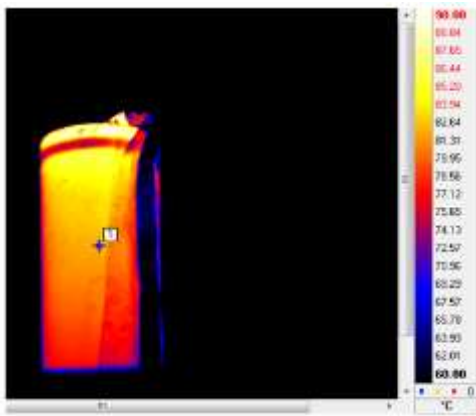


Fig. 11. Thermal image during 6 A overcharging of 18650 2.2 Ah NMC battery.

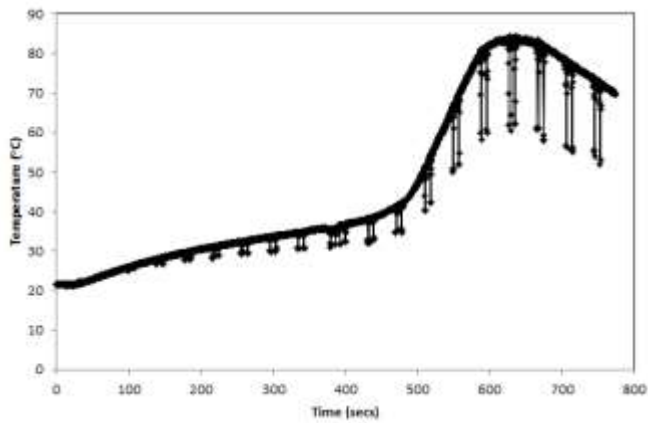


Fig. 12. Temperature reading from point 1 during 6 A overcharging of 18650 2.2 Ah NMC battery.

Tomography:

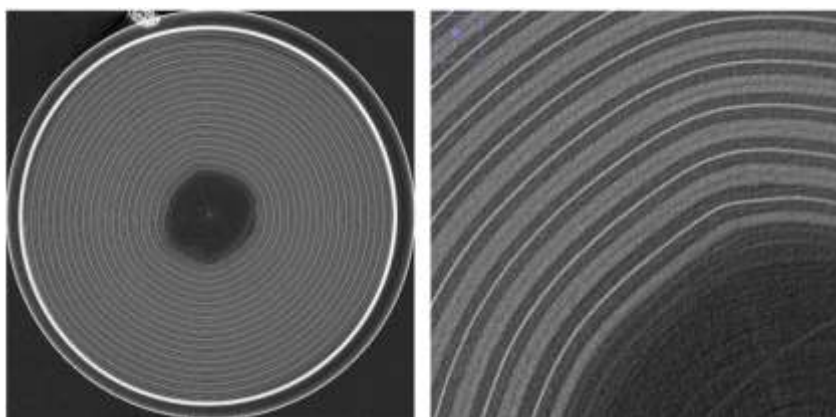


Fig. 13. Tomograph of 2.2 Ah NMC 18650 cell before overcharge abuse test. Tomograph of 2.2 Ah NMC 18650 cell before overcharge abuse test.

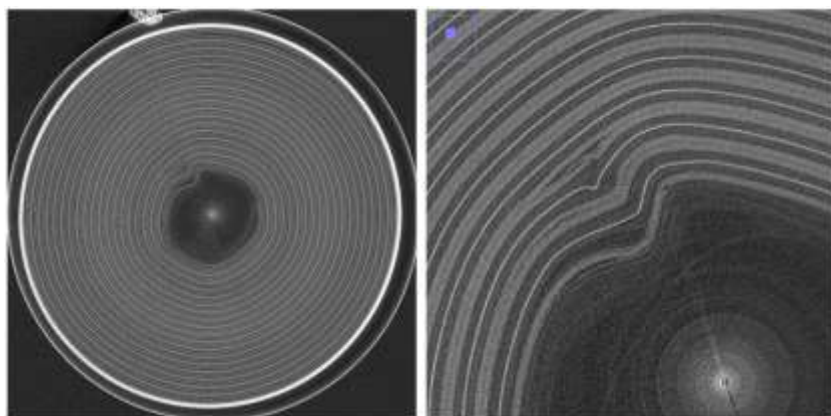


Fig. 14. Tomograph of 2.2 Ah NMC 18650 cell after overcharge at 6 A for ca. 700 s. Zoomed tomograph showing breakdown of electrode material. The formation of a gas pocket at the separator region indicated the oxidation of electrolyte material.

Comments:

16 tomographies captured the progression of this degradation. Rapid heat was observed after ca. 500 s potentially caused by exothermic electrolyte degradation reactions. The lack of internal support in the 2.2 Ah NMC cell allowed the inward collapse of the electrode material, an occurrence which may have been prevented by having an internal cylindrical support to keep the contents compressed. It is suspected that the PTC activated at the higher temperatures discontinuing the current flow and further overcharge.

Test G4

File name: NMC_charge_a [1-5]

Conditions

2.2 Ah NMC Charge from 3 V (discharged state) at 10 A. Slow tomo.

Results

Temperature at cap rose rapidly. After about 50 secs the current stopped. Experiment was stopped and battery was allowed to cool down before repeating the experiment. Repeated 5 times. PTC limited effect of rapid charge.

Electrical (repeated 5 times):

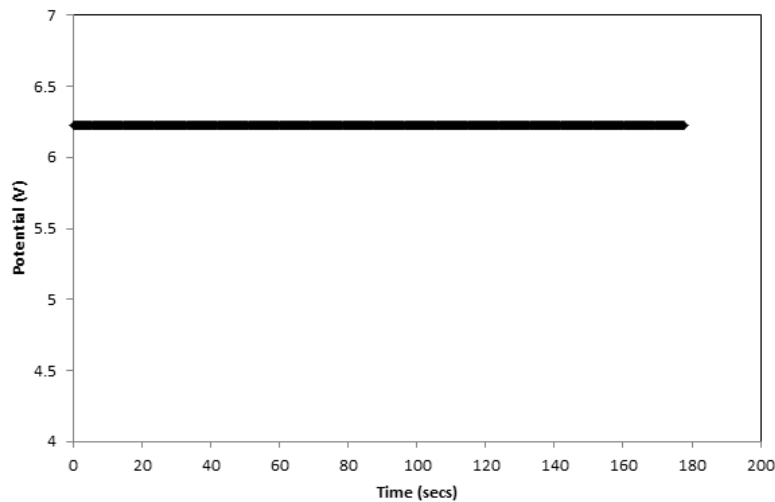


Fig. 15. Potential curve during charging. There appears to be an error in the readings for this test.

Thermal (repeated 5 times):

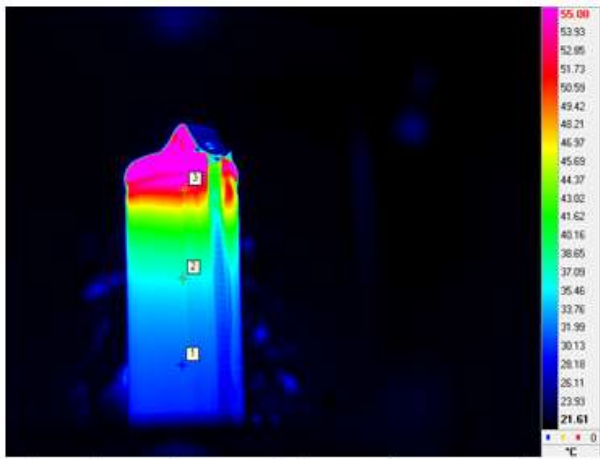


Fig. 16. Thermal image during rapid charging of 18650 2.2 Ah NMC battery

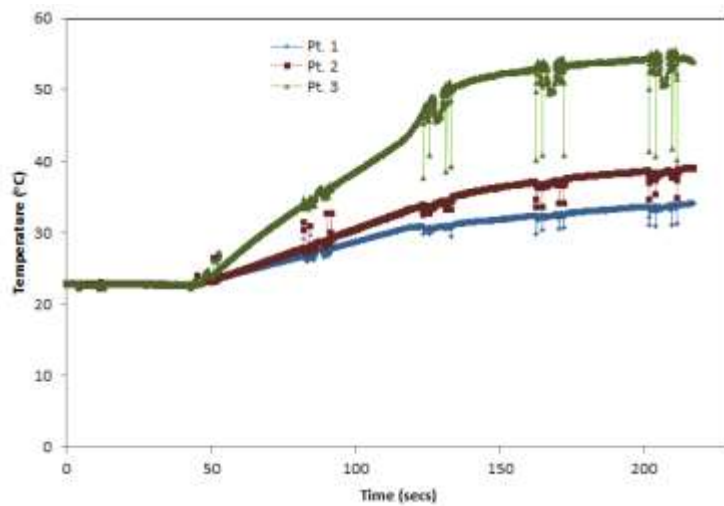


Fig. 17. Temperature at the three points along the batteries surface in the previous image during heating.

Tomography:

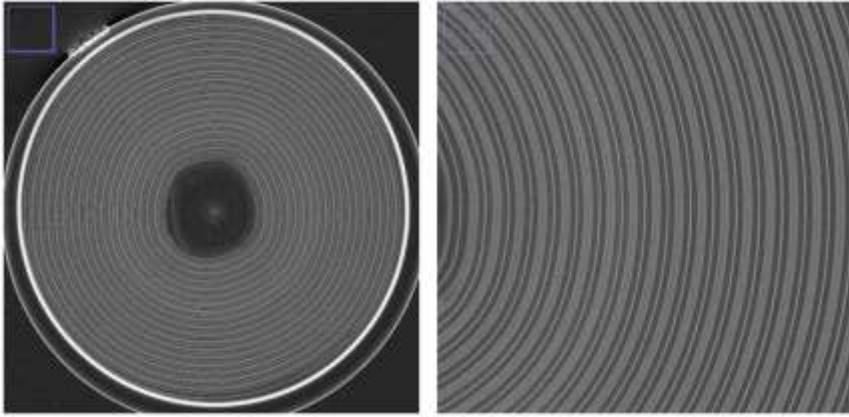


Fig. 18. Tomograph showing the state of a 2.2 Ah 18650 NMC battery after the first charge.
Tomograph showing a focused region of a 2.2 Ah 18650 NMC battery after the first charge.

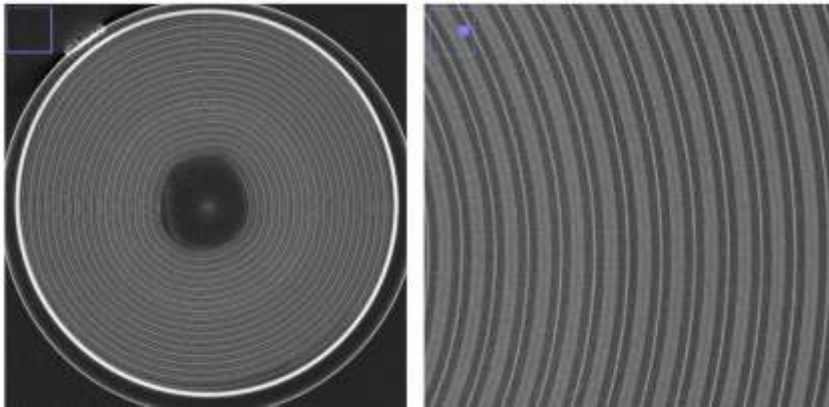


Fig. 19. Tomograph showing the state of a 2.2 Ah 18650 NMC battery after the fifth charge.
Tomograph showing a focused region of a 2.2 Ah 18650 NMC battery after the fifth charge.

Comments:

No noticeable change was seen over the 5 rapid charging processes. The battery was operated within the recommended operating voltages and the PTC device prevented overheating, therefore no gas generation was expected. Applying DVC to sequential images may reveal non-uniform expansion of the electrode material. During rapid charging it is expected that electrode swelling would mostly occur nearest the surface causing uneven strain fields throughout the NMC electrode material. The magnitude of swelling being greater near the surface would indicate lithium diffusion induced strain fields.

Test O₁

File name: NMC_Ch_120C_a [& b]

Conditions

Heat to ca. 120 °C (Gun 2 cm away from battery at 400 °C) until venting.

Results

Battery reached about 160 °C before venting. Expected SEI breakdown, gas generation - venting of gases and electrolyte.

Thermal:

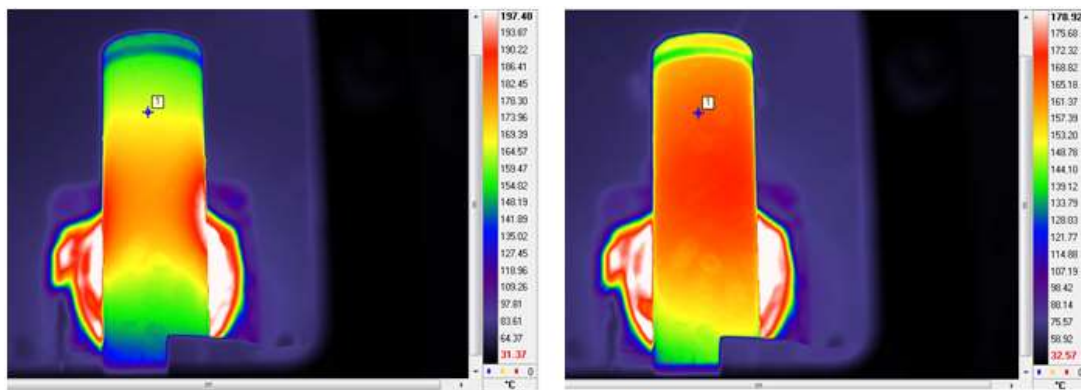


Fig. 20. Thermal image during heating of 18650 2.6 Ah NMC battery. Image is prior to venting.
Thermal image during heating of 18650 2.6 Ah NMC battery. Image taken after venting and heat gun turned off.

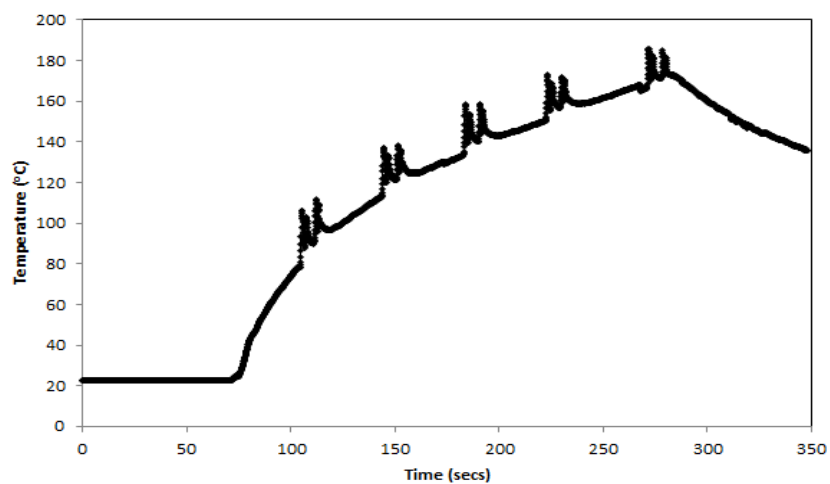


Fig. 21. Temperature at point 1 during heating of 18650 2.6 Ah NMC battery.

Tomography:

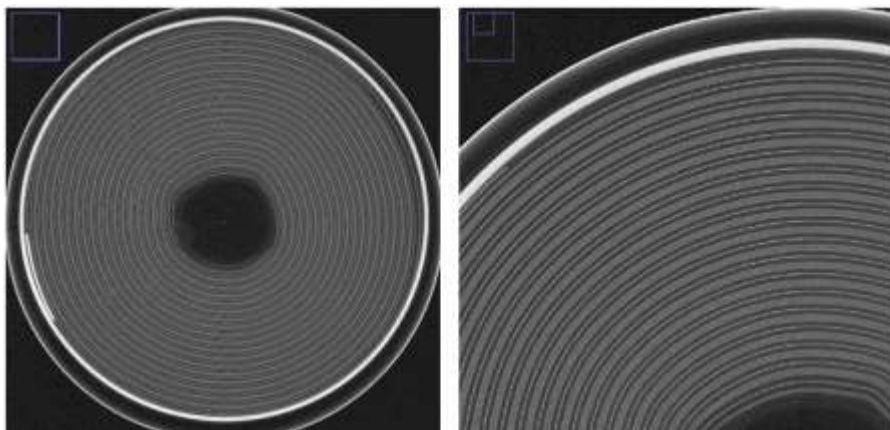


Fig. 22. Tomograph of 2.2 Ah NMC 18650 battery before thermal abuse test. Tomograph of 2.2 Ah NMC 18650 battery showing region of interest before thermal abuse test.

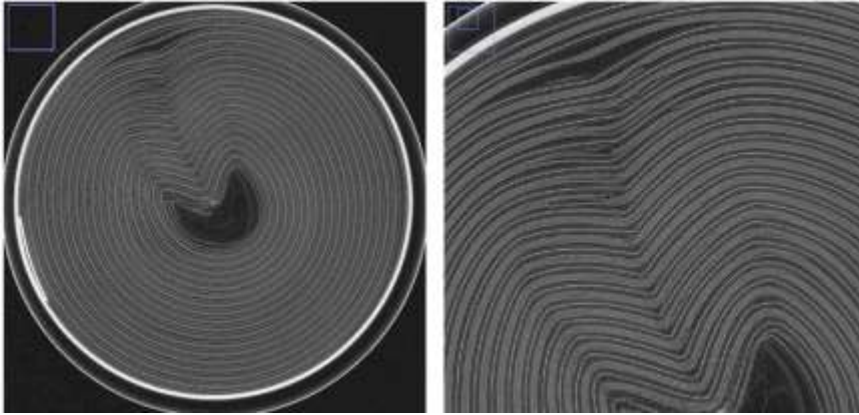


Fig. 23. Tomograph of 2.2 Ah NMC 18650 battery after thermal abuse test (after venting). Tomograph of 2.2 Ah NMC 18650 battery showing region of interest after thermal abuse test showing the presence of a gas pocket and consequent collapsed of the electrode material.

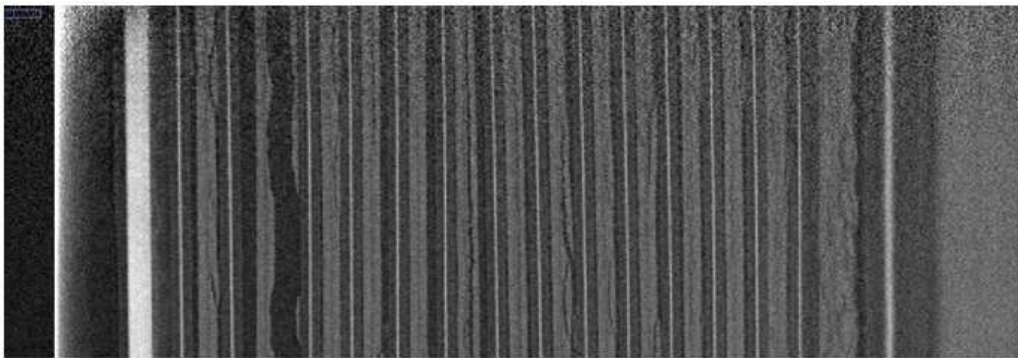


Fig. 24. Side view tomograph of 2.2 Ah NMC 18650 battery after thermal abuse test showing the presence of a gas pockets between the electrode layers.

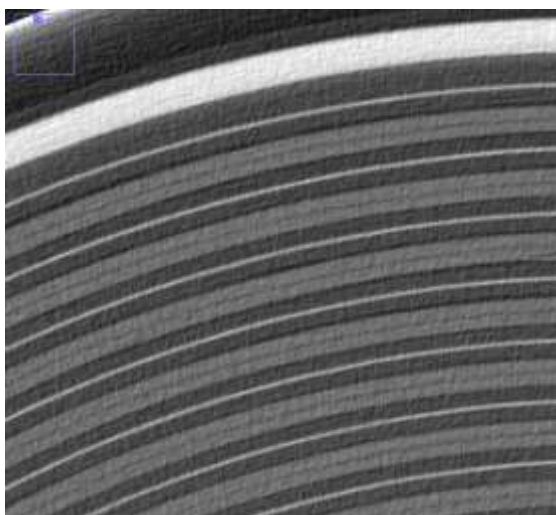


Fig. 25. Tomography of region of interest showing the formation of a thin gas pocket between the electrodes.

Comments:

9 tomographies were taken. The dramatic changes occurred over a single tomography (where venting occurred). In the tomographies leading up to venting a thin radial-laminar gas pocket can be seen spreading between the electrode materials, Fig. 25. DVC could be used to develop a strain profile on the electrode material over time which would highlight the initiation, propagation and effects of the gas pocket formation. The collapse of the electrode material into the centre could potentially have caused short-circuiting along the line of collapse.

The sudden pressure release during venting could have caused the structural collapse. With the sudden release of pressure, the radial-laminar gas pockets could have funnelled into a path of least flow resistance causing a rapid expansion in the region as the gaseous phase intrudes upwards along the delaminated regions, similar to the formation of a diapir in geology. For simplicity, this potential phenomenon will henceforth be referred to as the '*diapir effect*'.

Again, this highlights an obvious design flaw of not keeping the electrode material compressed/constrained.

Test O₂

File name: CR2_HG

Conditions

Battery was carried on from previous experiment attempting to rapidly overcharge battery. PTC quickly prevented this which left the battery at its nominal temperature. The CR2 battery in its charged state was heated to ca. 180. Heat gun set at 480 °C at ca. 2 cm from battery. Fast tomographies were taken.

Results

Cable came loose during experiment making the thermal readings difficult to capture during rotation periods. Battery exploded at ca. 180 °C. Expected SEI breakdown, separator melts, internal short, Li melts - venting, spitting and potentially sparks from the escaping molten Li.

Thermal:

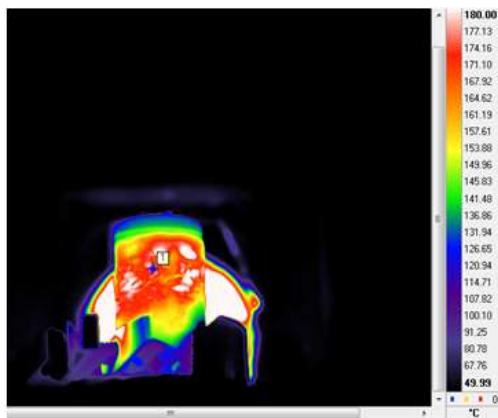


Fig. 26. Thermal image of CR2 battery during heating.

Test O₃

File name: CR2_120C_a [& b]

Conditions

Slower than previous. Heat a fully charged battery to ca. 180 °C. Heat gun set at 400 °C at ca. 2 cm from battery.

Results

Battery reached ca. 160 °C before venting and 200 °C before eruption. Metallic liquid seen emerging from the cap. Lots of dynamics in the data.

Thermal:

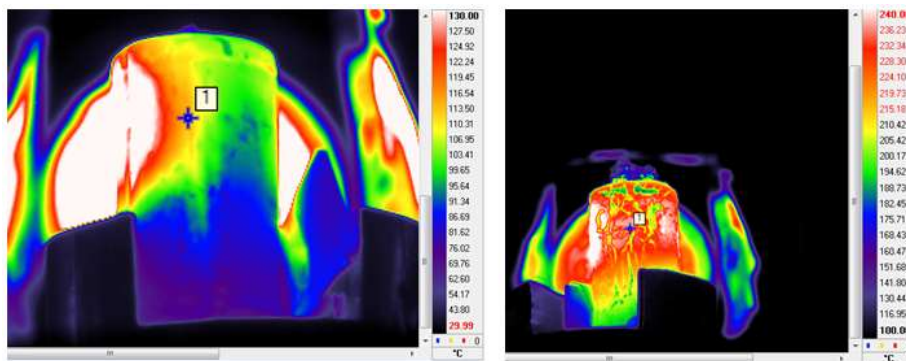


Fig. 27. Thermal image of CR2 battery during thermal abuse testing prior to venting. Thermal image of CR2 battery during thermal abuse after venting. Metallic liquid is seen bubbling from the cap of the battery.

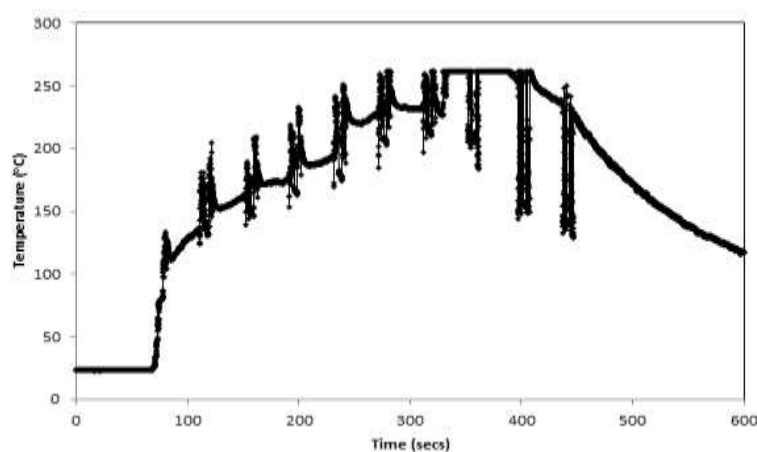


Fig. 28. Temperature at point 1 during thermal abuse of Duracell CR2 battery.

Tomography:

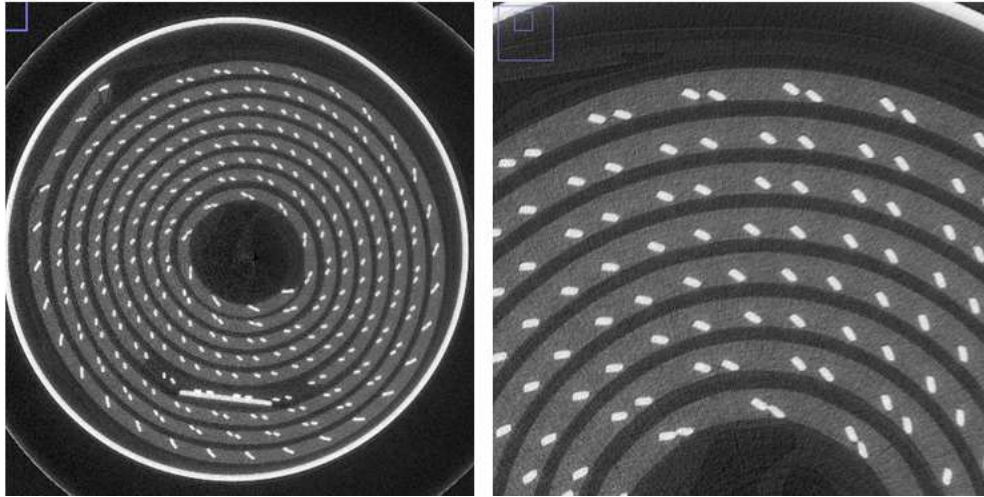


Fig. 29. Tomograph showing Duracell CR2 battery before the thermal abuse test. Tomograph showing Duracell CR2 battery showing a region of interest before the thermal abuse test.

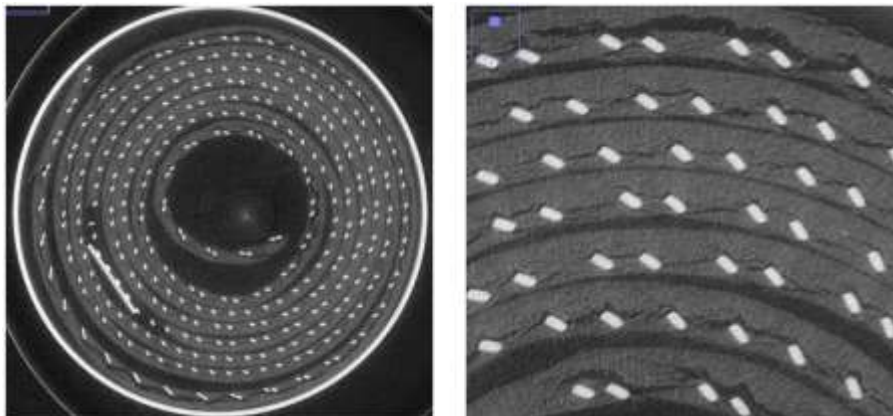


Fig. 30. Tomograph showing Duracell CR2 battery during the thermal abuse test before thermal runaway. Tomograph showing Duracell CR2 battery showing region of interest during the thermal abuse test before thermal runaway.

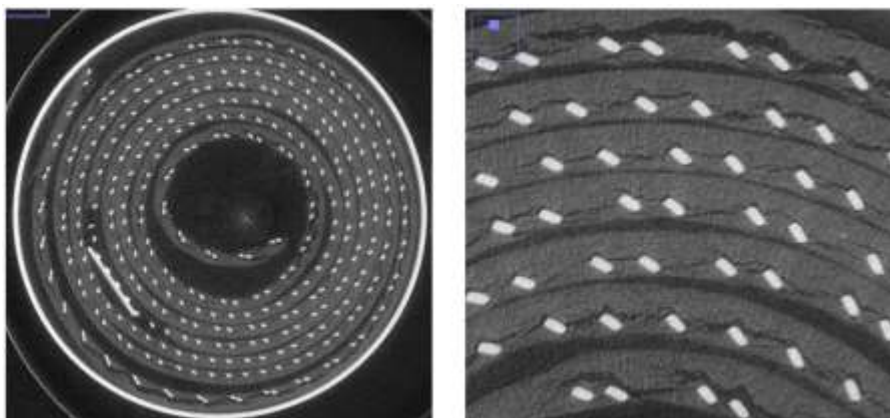


Fig. 31. Tomograph showing Duracell CR2 battery during the thermal abuse test before thermal runaway. Tomograph showing Duracell CR2 battery showing region of interest during the thermal abuse test before thermal runaway.

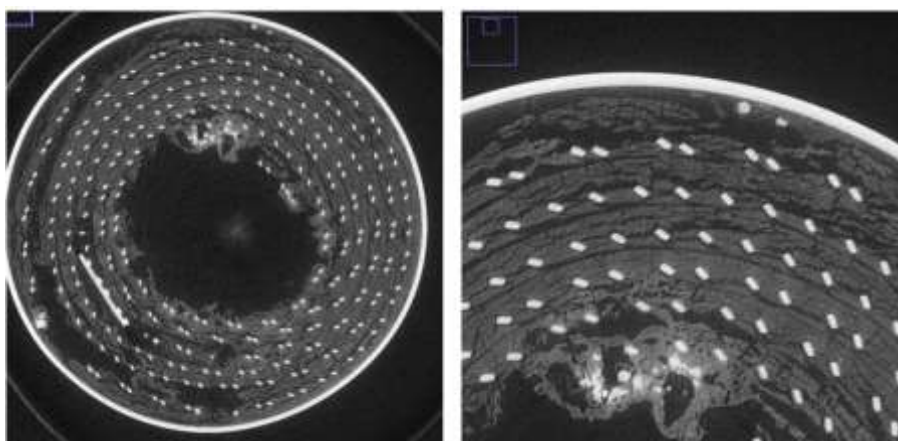


Fig. 32. Tomograph showing Duracell CR2 battery during the thermal abuse test after thermal runaway. Tomograph showing Duracell CR2 battery showing region of interest during the thermal abuse test after thermal runaway.

Comments:

The MnO_2 electrode material appears to swell at an early stage of heating. The separator is expected to melt at ca. 120-150 °C which could have caused a short circuit opening a path for lithiation to occur. The consequent rapid swelling of the MnO_2 material may have been the

cause of the crack propagation. The swelling would result in unravelling of the current collecting mesh causing detachment between the mesh and the MnO_2 .

A metallic liquid started to bubble out of the cell after reaching ca. 200 °C. After thermal runaway, highly absorbing globules appear. At first sight they appear to have a similar attenuation as the nickel current collecting mesh. This could easily be verified by isolating the phase and checking whether the mesh was still completely intact. The melting point of nickel is 1455 °C which could provide an insight into the internal temperatures reached during thermal runaway. Ribiere et al. reported temperature of MnO_2 batteries reaching over 1000 °C during thermal runaway.⁷¹ The battery remains could also be dissected and samples analysed for compositions.

Test O4

File name: A123Ch_120CHG [&] A123_Ch_120C_b

Conditions

Heat fully charged battery (4.2 V) to 120 °C. Gun 2 cm away from battery at 400 °C.

Results

A123 vented at 120 °C. Heat gun turned off. Spewing and bubbling continued for ca. 5 mins keeping at ca. 115 °C. Battery cooled down thereafter.

Thermal:

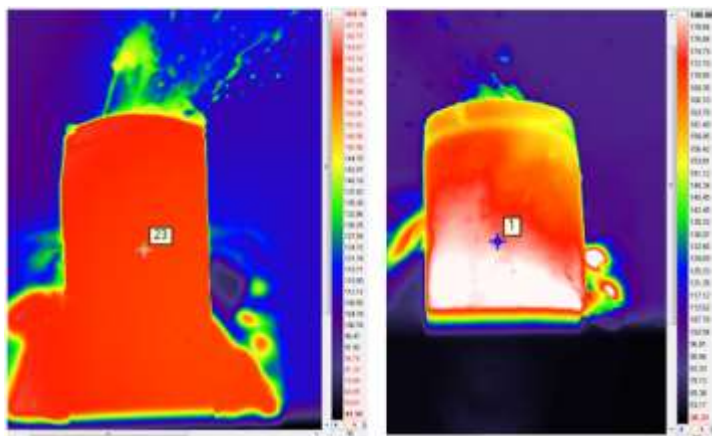


Fig. 33. Thermal image of 18650 A123 FePO_4 battery during venting. Venting occurred after 340

secs. (Temperature peaked for $A_{123}Ch_{120}CHG$) Thermal image of 18650 $A_{123}FePO_4$ battery during venting. Venting occurred after 405 secs. ($A_{123}Ch_{120}C_b$)

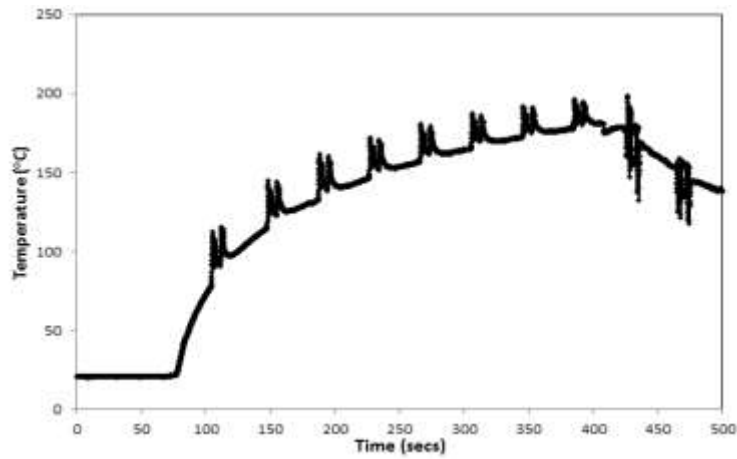


Fig. 34. Temperature at point 23 during thermal abuse of 18650 $A_{123}FePO_4$ battery. Venting occurs after 405 s where the temperature fluctuation occurs.

Tomography:

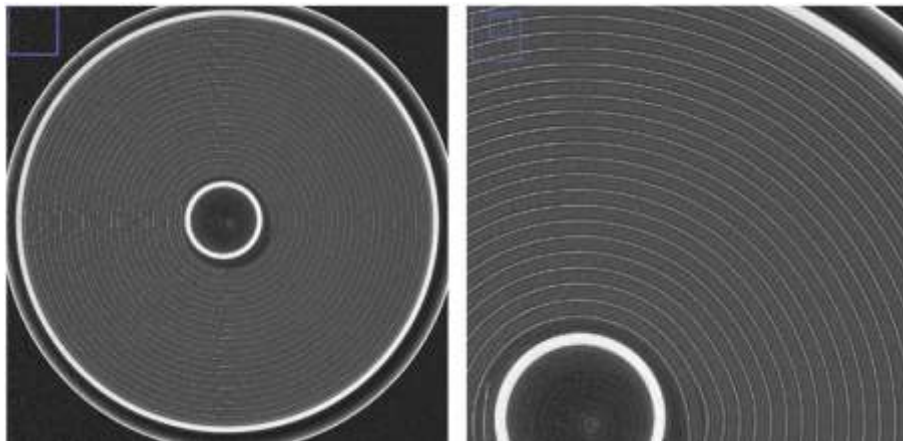


Fig. 35. Tomograph of $FePO_4 A_{123}$ 18650 battery before thermal abuse test. Tomograph showing region of interest of $FePO_4 A_{123}$ 18650 battery before thermal abuse test. Time = 0.

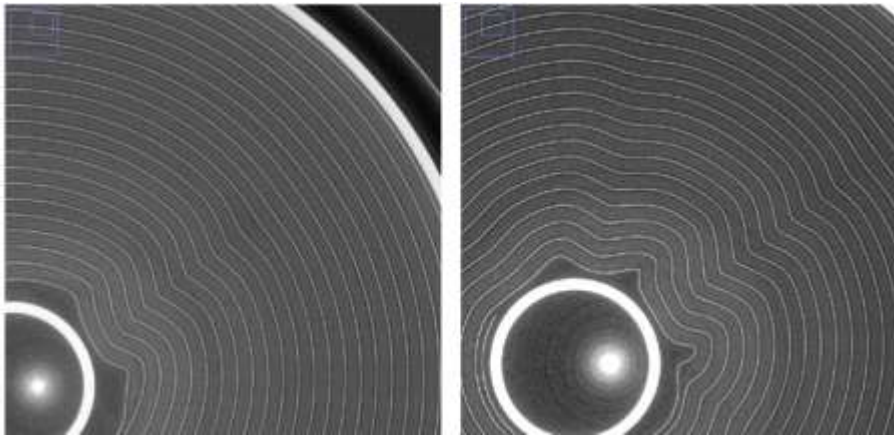


Fig. 36. Tomograph showing gradual collapse of electrode materials during thermal abuse test. Time = ca. 150 secs. Tomograph showing gradual collapse of electrode materials during thermal abuse test. Time = ca. 200 secs.

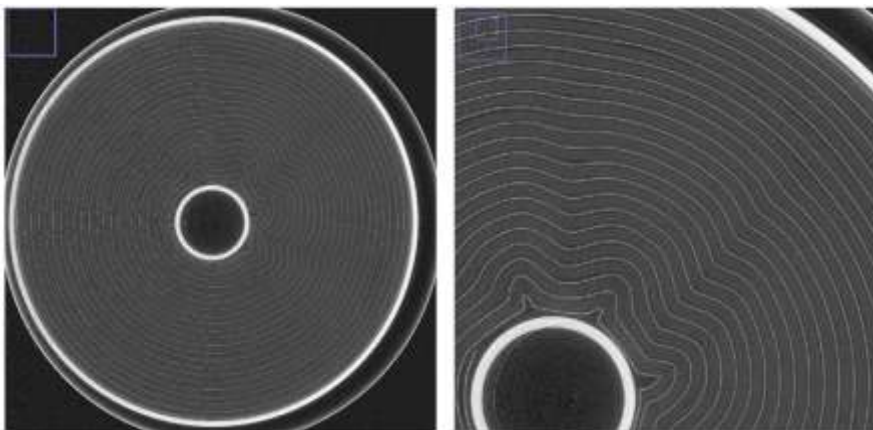


Fig. 37. Tomograph of FePO_4 A123 18650 battery after thermal abuse test. Tomograph showing region of interest of FePO_4 A123 18650 battery after thermal abuse test.

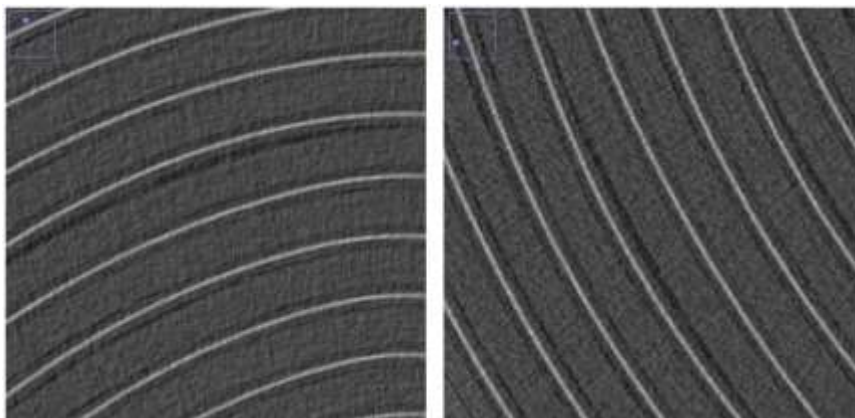


Fig. 38. Tomograph showing evidence of radial laminar gas pockets forming at the interface between the graphite and FePO_4 electrodes. Tomograph showing evidence of radial laminar gas pockets forming at the interface between the graphite and FePO_4 electrodes.

Comments:

A time dependent strain map could potentially be developed using DVC. The progression of gas pocket formation and electrode collapse could be linked to the temperature of the battery. The radial laminar gas pockets appear to form between the FePO_4 and graphite electrodes indicating that the evaporating electrolyte delaminates the separator region from the electrode, reducing the ionic conductive area between the electrodes.

Unlike the 18650 LG NMC cells, the A123 has an internal cylindrical support which mitigates the potential '*diapir effect*' due to the sudden release of pressure during venting. The A123 design appears to maintain the mechanical integrity cell much better than the LG cells during failure.

Test O5

File name: LiPo_Charge3A_a [& b & c]

Conditions

LiPo Overcharge from nominal at 3 A until fail. Slow tomo.

Results

Image with large black artefact. Large black artefact believed to be due to the misalignment of the cage with the beam.

Electrical:

The 40 second period over which swelling, rupture and thermal runaway occurs can be identified by the distortions in the potential curve.

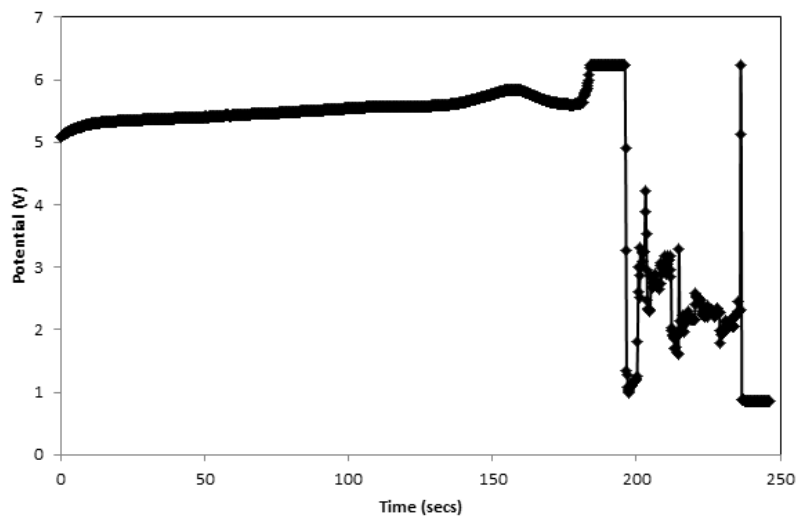


Fig. 39. Cell potential during overcharge of LiPo cells.

Thermal:

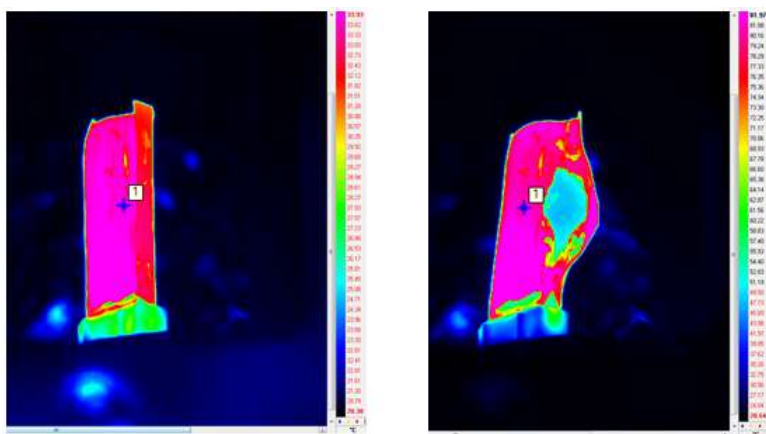


Fig. 40. Thermal image of LiPo battery during overcharging abuse test at 3 A. Thermal image of LiPo battery after pouch rupture during overcharging abuse test at 3 A.

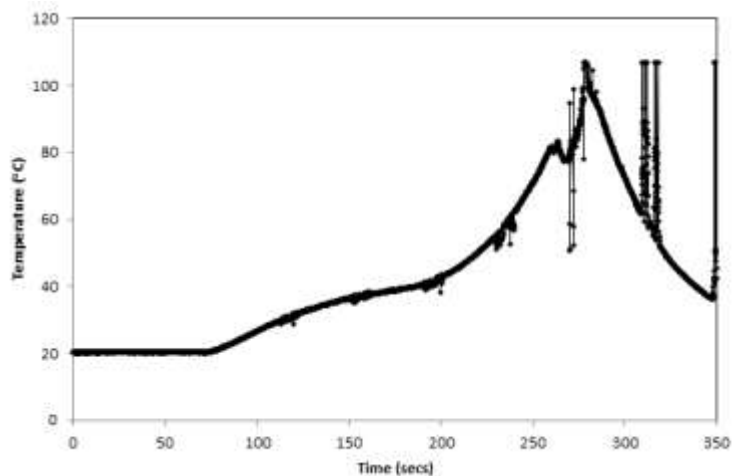


Fig. 41. Temperature at point 1 in LiPo battery during overcharging abuse test at 3 A. The sudden dip in temperature at 260 s is the point of pouch cell rupture. The surface of the cell reaches a maximum of ca. 110 °C before exploding.

Tomography:

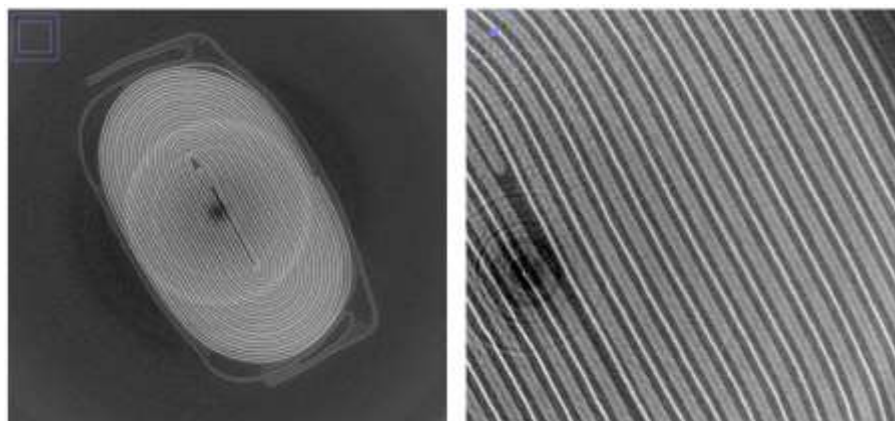


Fig. 42. Tomograph of Turnigy 160 mAh LiPo cell before overcharge abuse test. Fig. 43. Tomograph showing region of interest of Turnigy 160 mAh LiPo cell before overcharge abuse test.

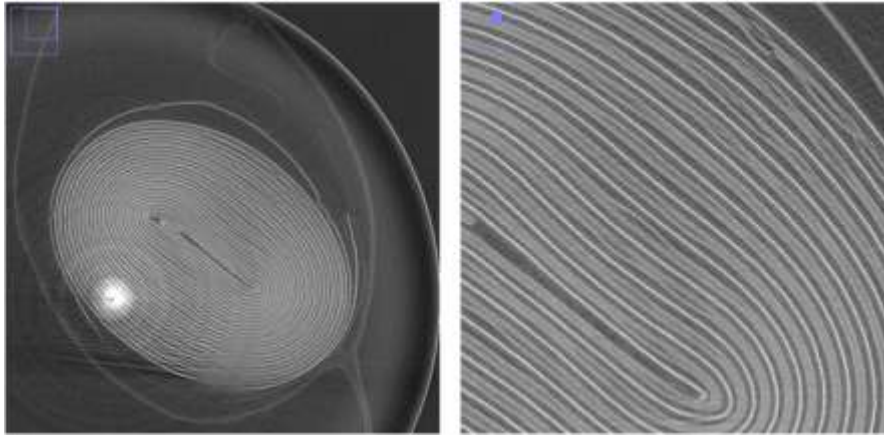


Fig. 44. Tomograph of Turnigy 160 mAh LiPo cell during overcharge abuse test of 3 A until fail. Tomograph showing region of interest of Turnigy 160 mAh LiPo cell during overcharge abuse test of 3 A until fail.

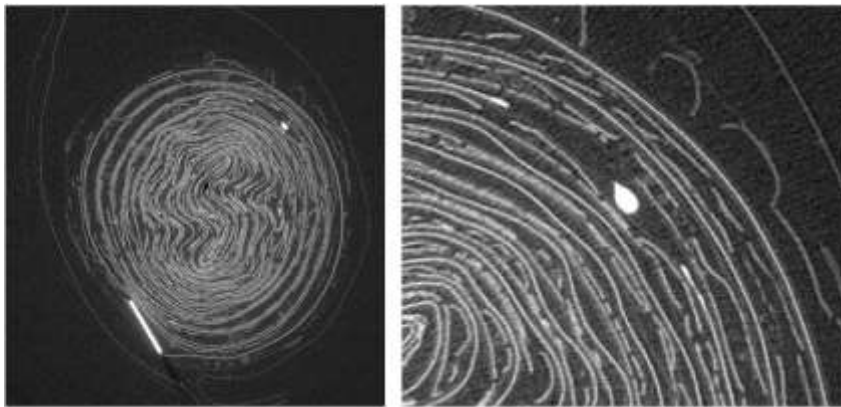


Fig. 45. Post-mortem tomograph of Turnigy 160 mAh LiPo cell after overcharge abuse test of 3 A until fail. Post-mortem tomograph showing region of interest of Turnigy 160 mAh LiPo cell after overcharge abuse test of 3 A until fail.

Comments:

During overcharge abuse tests, it is expected that the oxidation of the electrolyte material will occur after ca. 4.7 V resulting in gas generation, pouch swelling and rupture. Delamination is seen between the electrode materials. The generated gas appears to seep out at the ends of the rolled cell and expands the pouch. Initially, the gas pocket formation appears to be most

severe around the straight regions whereas at the bends there is little evidence of electrode breakdown or gas pocket formation. At the bends in the cell, the rolled cell materials will be under higher tension than the straight regions which appears to help maintain structural integrity during electrical abuse.

The point of cell rupture can be seen from the sudden drop in temperature (ca. 5 °C) of the cell. This is expected to be as a result of the Joule-Thompson effect and can be seen for each of the battery types directly after venting. The Joule-Thomson effect for venting batteries has also been seen by Golubkov et al.⁷⁵.

When thermal runaway occurred, the pouch cell fell out of sight of the thermal camera and X-ray. The cell was repositioned after the test for a post-mortem scan. Evidence of the copper electrode melting is seen. This indicates that local temperatures may have reached > 1000 °C.

Test O6

File name: LiPo_Heat_120C [& b]

Conditions

Heat to 120 °C. Heat gun pointed at battery (2 cm away at 300 °C).

Results

Battery heated rapidly, swelled and burst. Artefact in the centre of the image – use different flat field during reconstruction.

Thermal:

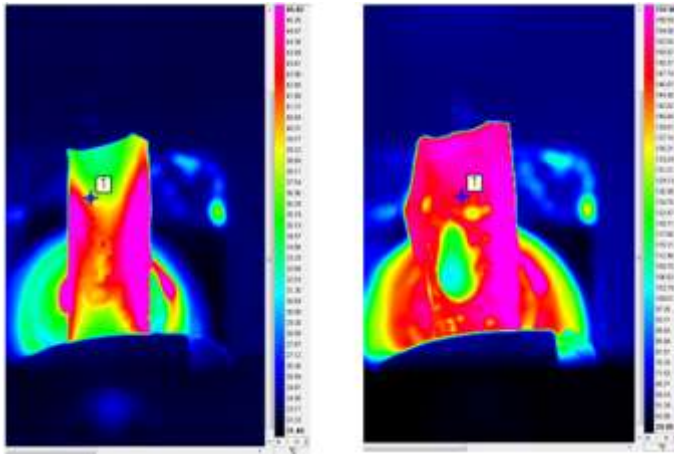


Fig. 46. Thermal image of LiPo cell during thermal abuse test. Thermal image of LiPo cell after venting during thermal abuse test.

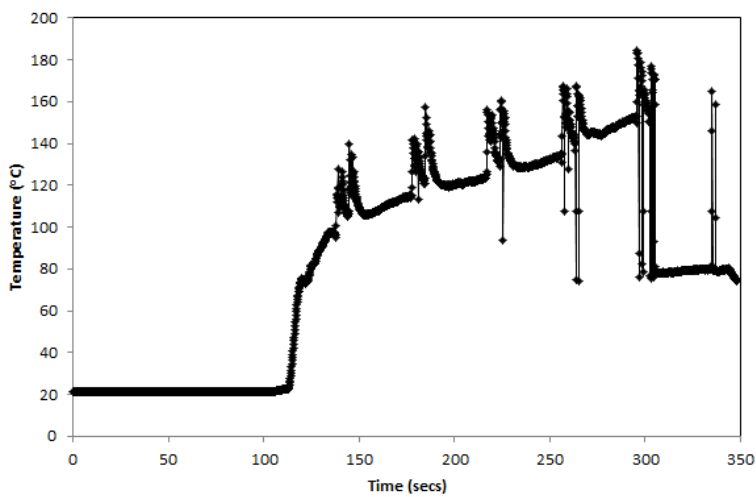


Fig. 47. Temperature at point 1 during thermal abuse testing of LiPo cell.

Tomography:

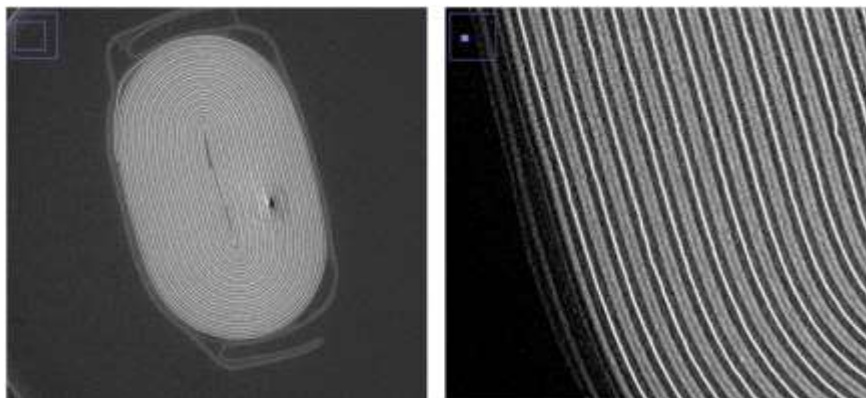


Fig. 48. Tomograph of Turnigy 160 mAh LiPo cell before thermal abuse test. Tomograph of Turnigy 160 mAh LiPo cell showing region of interest before thermal abuse test.

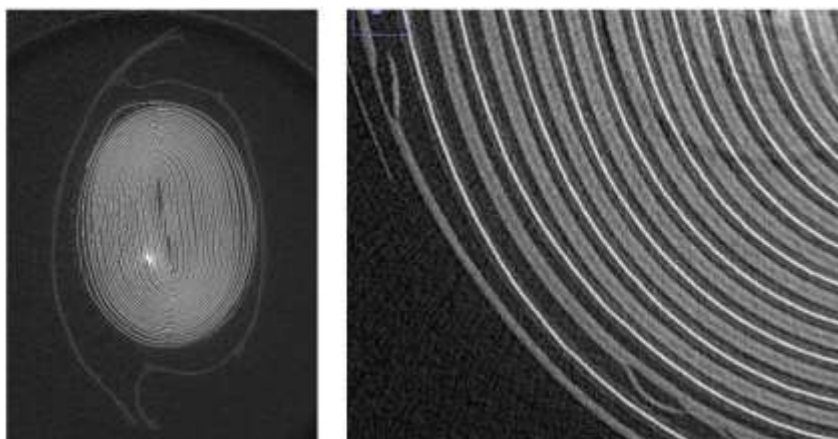


Fig. 49. Tomograph of Turnigy 160 mAh LiPo cell after thermal abuse test. Tomograph of Turnigy 160 mAh LiPo cell showing region of interest after thermal abuse test.

Comments:

The maximum temperature reached was ca. 160 °C. Below this temperature the SEI layer is expected to breakdown and the electrolyte may decompose (depending on the composition – proprietary). This would explain the apparent separation of the carbon and Li_xCoO_2 (to be verified) electrode materials. The swelling of the pouch may be attributed to the seeping of decomposition gaseous products out of the

Test O7

File name: CR2_Ch_Sl_a_1

Conditions

Overcharge the battery at 1 A. Slow tomo.

Results

Interesting potential curve. Temperature reached ca. 80 °C before venting and cooling. After cooling voltage returned to normal and slowly increased over time - possible due to lithium diffusion of lithium plating.-worth testing in lab.

Electrical:

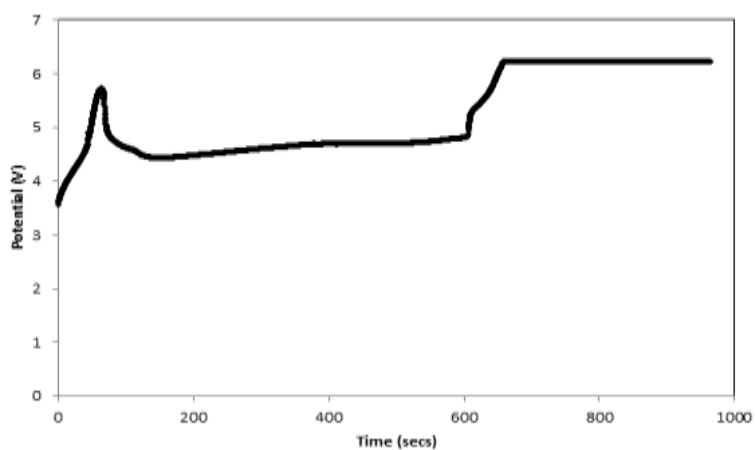


Fig. 50. Cell potential during overcharge of CR2 battery.

Thermal:

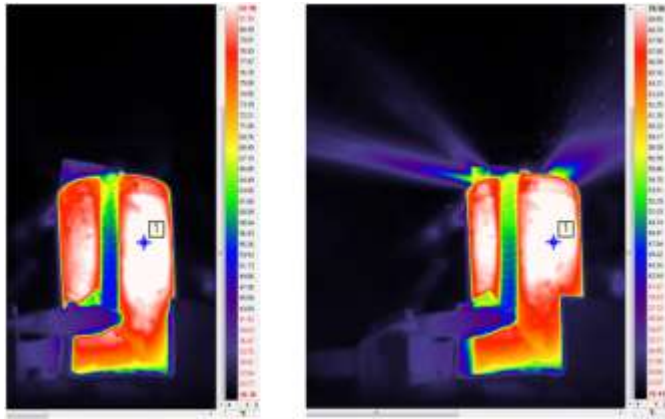


Fig. 51. Thermal image during overcharging of Duracell CR2 battery at 1 A. Thermal image showing venting of Duracell CR2 battery during overcharge abuse test.

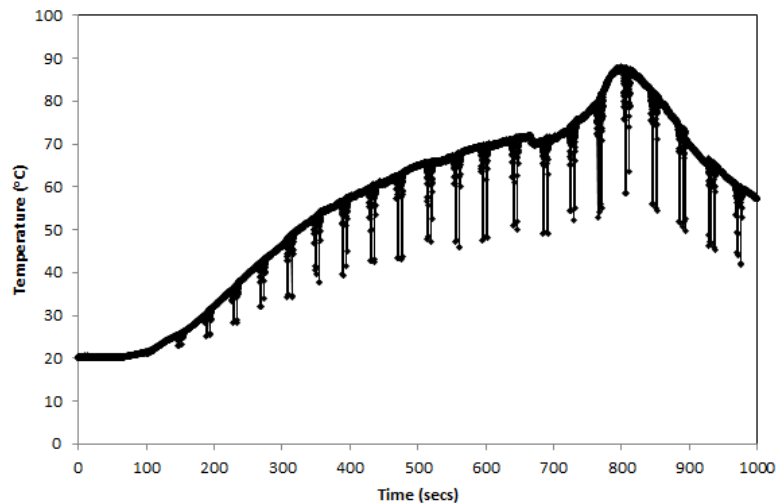


Fig. 52. Temperature reading from point 1 during overcharge of Duracell CR2 battery at 1 A. The slight dip in temperature at ca. 680 secs shows the point at which the cell vents.

Tomography:

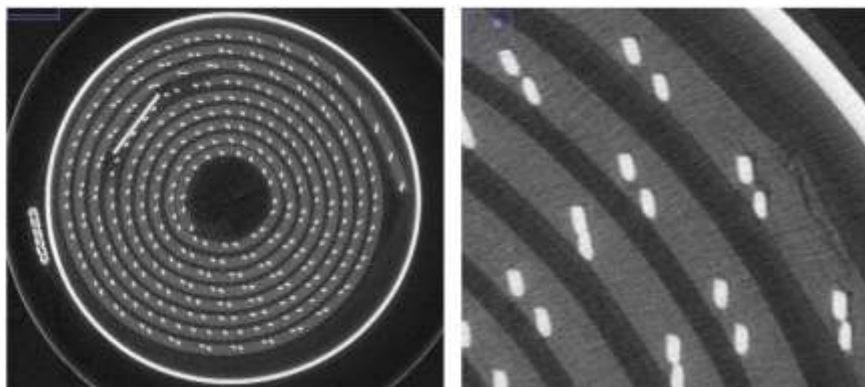


Fig. 53. Tomograph of Duracell CR2 battery before overcharge abuse test at 1 A. Tomograph showing region of interest of Duracell CR2 battery before overcharge abuse test at 1 A.

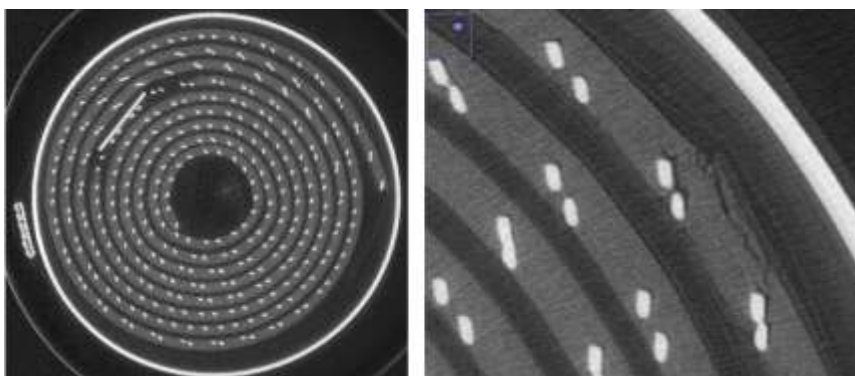


Fig. 54. Tomograph of Duracell CR2 battery after overcharge abuse test at 1 A. Tomograph showing region of interest of Duracell CR2 battery after overcharge abuse test at 1 A.

Comments:

24 tomographies captured this development. A thin but definite grey layer is seen on the surface of the MnO_2 electrode after the overcharge abuse test. This is likely to be the separator layer which separates from the surface of the MnO_2 electrode as the MnO_2 contracts during delithiation.

Test O8

File name: CR2_ch

Conditions

Overcharge the battery at 3 A. Fast tomo.

Results

Fast tomo limited experiment to 17 s during which time no significant change was observed in the images.

Thermal:

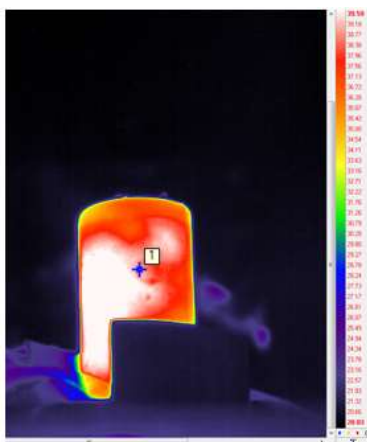


Fig. 55. Thermal image of rapid overcharge abuse test of Duracell CR2 battery.

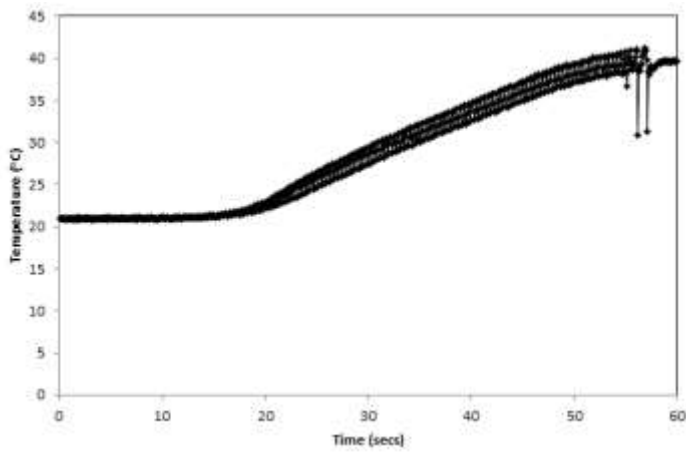


Fig. 56. Temperature at point 1 during rapid overcharge of Duracell CR2 battery.

Tomography:

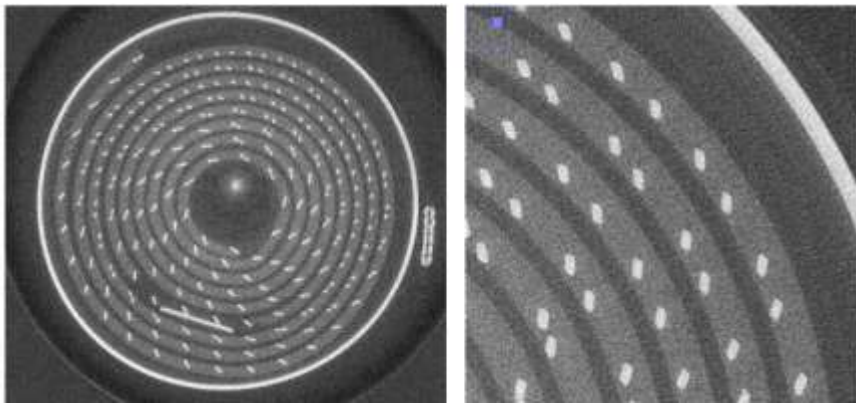


Fig. 57. Tomograph of Duracell CR2 battery after overcharge abuse test at 3 A captured with fast tomography. Tomograph showing region of interest of Duracell CR2 battery before overcharge abuse test at 3 A captured with fast tomography.

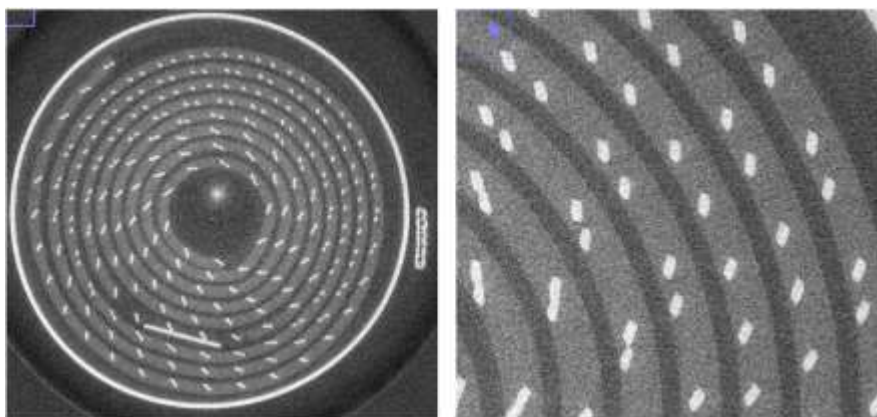


Fig. 58. Tomograph of Duracell CR2 battery after overcharge abuse test at 3 A captured with fast tomography. Tomograph showing region of interest of Duracell CR2 battery after overcharge abuse test at 3 A captured with fast tomography.

Comments:

Fast tomography captured 38 tomographies over 17 s during the overcharging abuse test. Each tomography consists of 500 projections instead of the usual 2000 which results in the images appearing more 'grainy'. There is no noticeable difference between the first and last tomography in this test.

Red

Electrical Abuse Test:

Test R₁

*File name: NMC_Ch_18oC_test1 [slow] & NMC_Ch_18oC_test4 [Fast]***

Conditions

Heat fully charged battery (4.2 V) to 180 °C. Heat gun set at 480 °C at ca. 1.5 cm from battery. Fast and slow tomos.

Results

Venting at early stage. Thermal runaway when battery reached about 250 °C after ca. 2 minutes. Thermal runaway and explosion. Formation of gas pockets observed in slow tomography. Thermal runaway captured and explosion captured in radiographs.

Thermal:

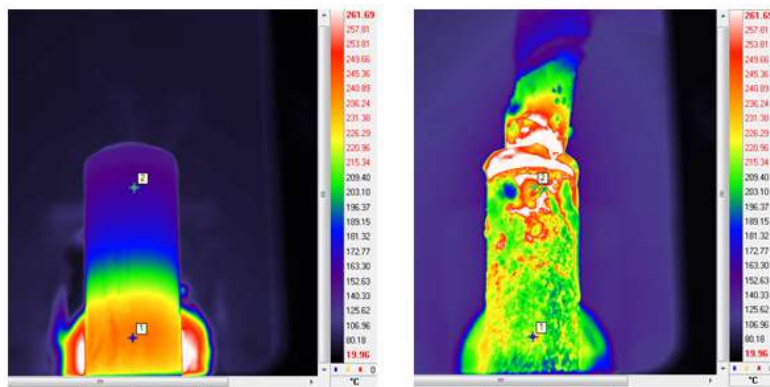


Fig. 59. Thermal image of 18650 2.6 Ah NMC battery during extreme thermal abuse. Thermal image of 18650 2.6 Ah NMC battery after thermal runaway and explosion during extreme thermal abuse. Complete ejection of internal material occurred.

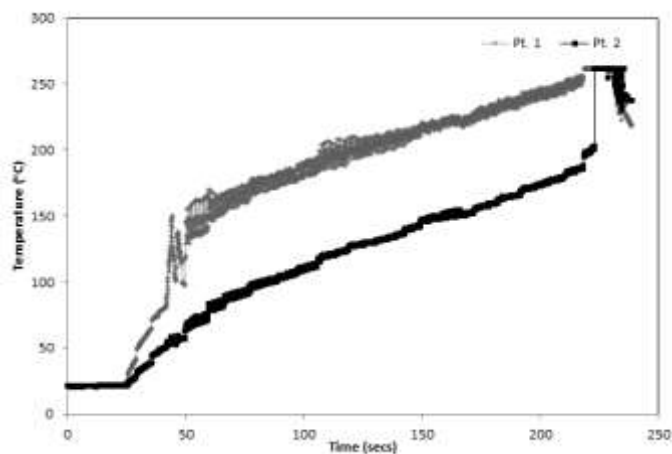


Fig. 60. Temperature at point 1 and 2 during extreme thermal abuse of 18650 2.6 Ah NMC batteries. Thermal camera readings were limited to 260 °C. The final temperature of the battery shell was not captured. The apparent presence of melted copper globules in the post mortem tomographies indicate that temperatures reached >1000 °C inside the battery casing.

Tomography:

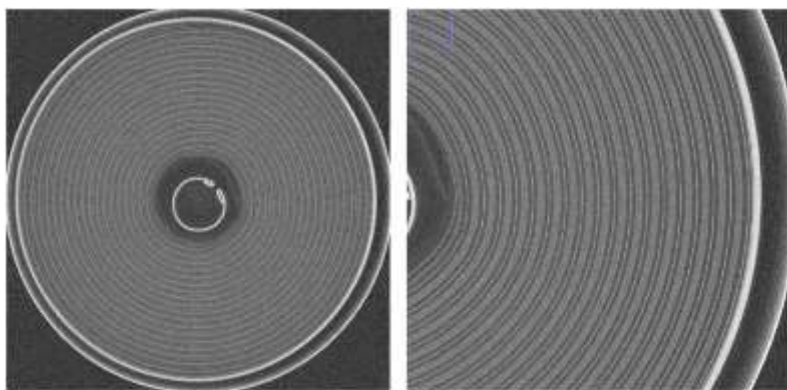


Fig. 61. Slow tomography tomograph showing LG 2.6 Ah NMC battery before thermal abuse test. Slow tomography tomograph showing region of interest of LG 2.6 Ah NMC battery before thermal abuse test.

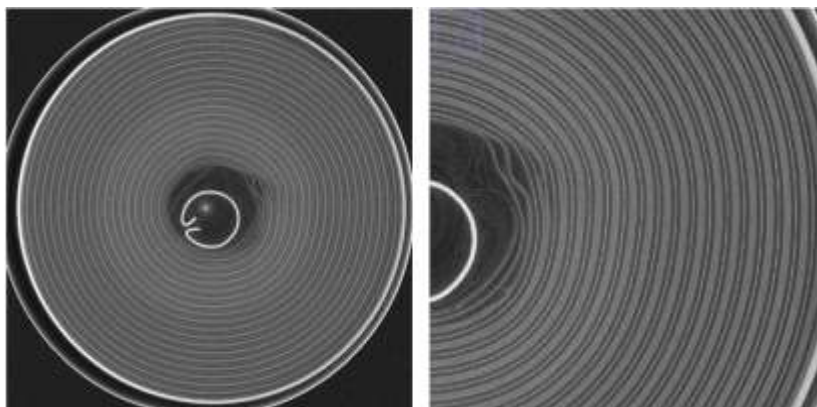


Fig. 62. Fast tomography tomograph showing the state of the battery 2 s before thermal runaway and explosion. Fast tomography tomograph showing the state of the battery in the region of interest 2 s before thermal runaway and explosion. Gas pockets appear to form in the inner regions of the electrode roll.

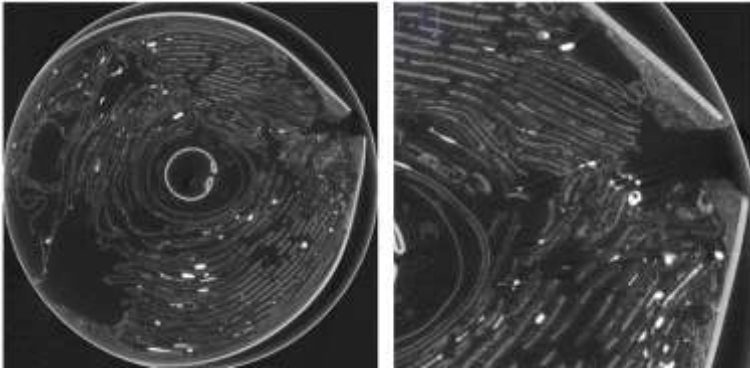


Fig. 63. Post-mortem tomograph showing the remnants of battery internals after thermal runaway. The side of the cell split open during failure. Post-mortem tomograph showing the region around the split in the shell casing after thermal runaway and explosion.



Fig. 64. Radiograph (side view) of the LG NMC 18650 battery showing the electrode material at the initiation of thermal runaway.

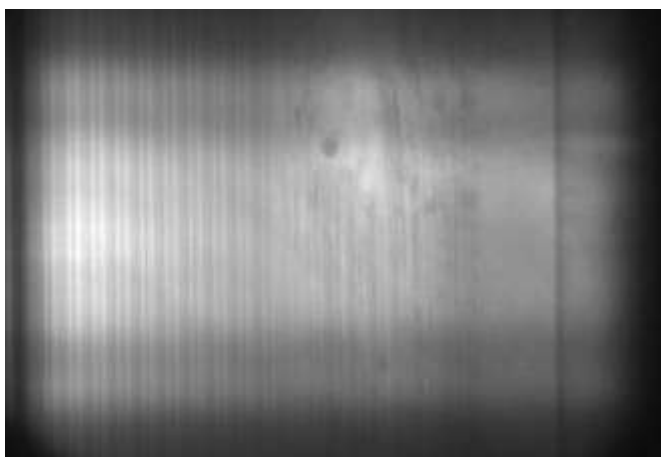


Fig. 65. Radiograph (side view) of the LG NMC 18650 battery showing the beginning of the breakup of electrode material during thermal runaway.

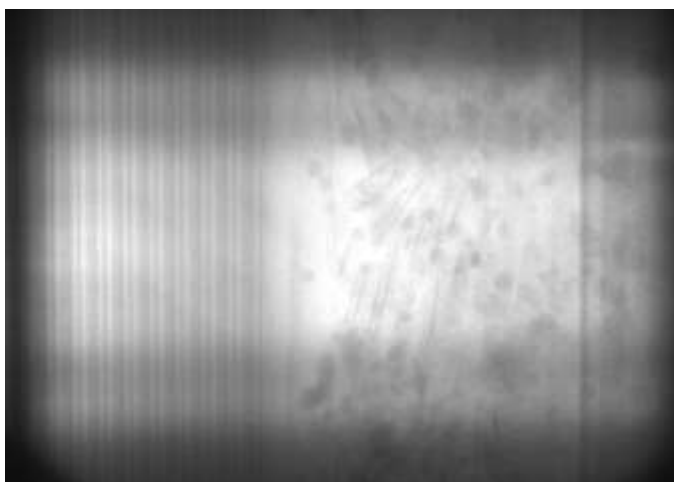


Fig. 66. Radiograph (side view) of the LG NMC 18650 battery showing the propagation of the breakup of electrode material during thermal runaway.

Comments:

The process of thermal runaway occurs over a short period of time, typically a few seconds⁷⁵. Fast tomography involved tomographies being taken every 0.4 s which was still not fast enough to capture the rapid break-down of materials associated with the propagation of thermal runaway, notably, the rapid formation of gaseous products from the thermally and electrochemically driven reactions. The tomographies taken during thermal runaway were spoiled by the extent of dynamic events which occurred over the 0.4 s of imaging. The rapid formation of gases and high temperature gradients would result in significant perturbations in the structure of the surrounding materials.

However, each tomography is reconstructed from 500 individual radiographs. The rapid progression of perturbations and runaway reactions was captured by the individual radiographs which were 0.0008 s apart. Hence, 2D radiograph images captured the progression of events at 1250 frames (radiographs) per second, three of which are shown in the figures above.

Thermal runaway occurred when the battery reached ca. 180 °C. The final temperature exceeded the set limit of the thermal camera. Golubkov et al.⁷⁵ reported surface temperatures of commercial NMC cells reaching in ca. 700 °C during thermal runaway. The post-mortem scans reveal what appear to be copper globules which indicate that internal temperatures may have reached in excess of 1085 °C, the melting point of copper.

Test R2

File name: NMC_7A_180C_a_charge [&] NMC_7A_180C_a_heat

Conditions

Overcharge at 7A to cut-off limit (ca. 5.3 V) then heat to ca. 180 °C with fast tomography. Slow tomo.

Results

Significant heating and current trip when the sample reached ca. 80 °C.

Very rapid thermal runaway and catastrophic explosion ~ 17 secs.

Electrical:

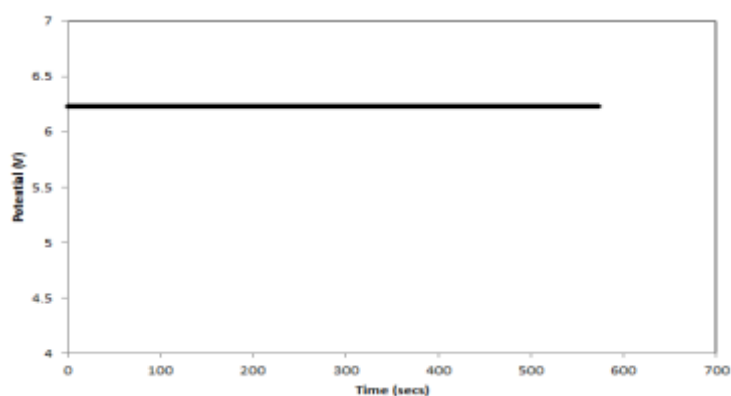


Fig. 67. Cell potential during overcharge. There appears to be an error in the readings.

Thermal:

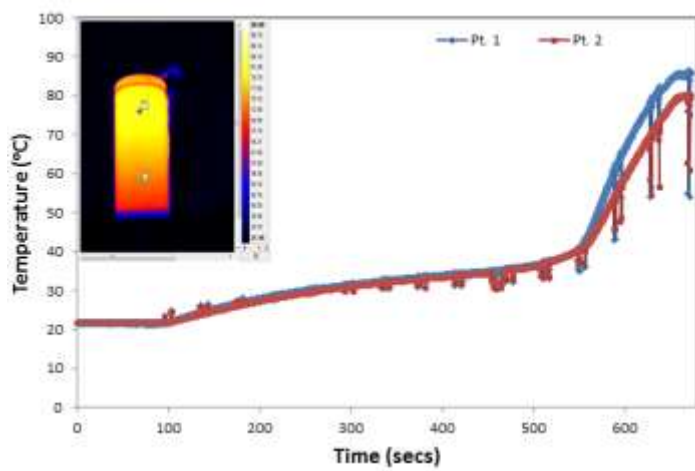


Fig. 68. Temperature of NMC cell during overcharge test.

Tomography:

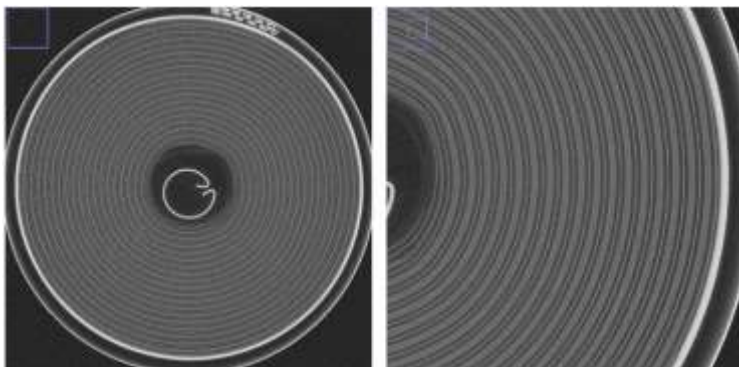


Fig. 69. Tomography of the 2.6 Ah 18650 NMC cell before thermal and electrical abuse test. Tomography showing a focused region of the 2.6 Ah 18650 NMC cell before thermal and electrical abuse test.

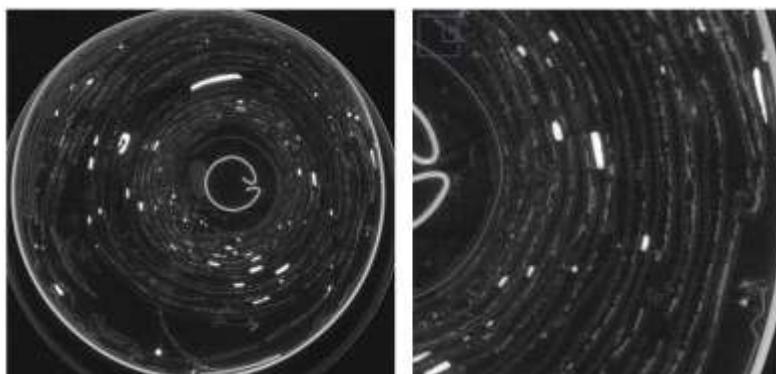


Fig. 70. Post-mortem tomograph showing the remnants of battery internals after overcharging at 7 A and heating above 150 °C. Post-mortem tomograph showing a focused region after overcharging at 7 A and heating above 150 °C.

Comments:

No noticeable change in the internal structure of the battery was noticed during the overcharging process. It's possible that lithium plating occurred but the high X-ray transparency of lithium may have prevented the occurrence from being observed. A similar post-mortem image to the overheating of a fully charged NMC cell was seen. There is evidence of copper globules indicating that internal temperatures reached in excess of 1085 °C. It's worth noting that thermal runaway occurred at a lower temperature than the fully charged NMC battery.

Of all the experiments performed the failure conditions in this experiment are the most unlikely to occur in reality. The experiment was not repeated in the interest of time.

Test R₃

File name: A123_Ch_180C_test [fast] & A123_180C_test2 [slow]

Conditions

Heat fully charged battery (4.2 V) to 180 °C. Heat gun set at 500 °C at ca. 1.5 cm from battery. Fast and slow tomos.

Results

Fast tomo: Venting at early stage. Thermal runaway when battery reached about 250 °C after ca. 4 minutes. Venting with liquid spewing soon followed by explosion with loud pop. Lots of dynamics leading up to explosion. Complete ejection of contents.

Slow tomo: Heating was different for fast and slow tomos. Constant spinning for fast tomo helped apply the heat uniformly. Slow tomo resulted in heat being focused on one side. The failure for slow tomo did not result in complete ejection.

Thermal:

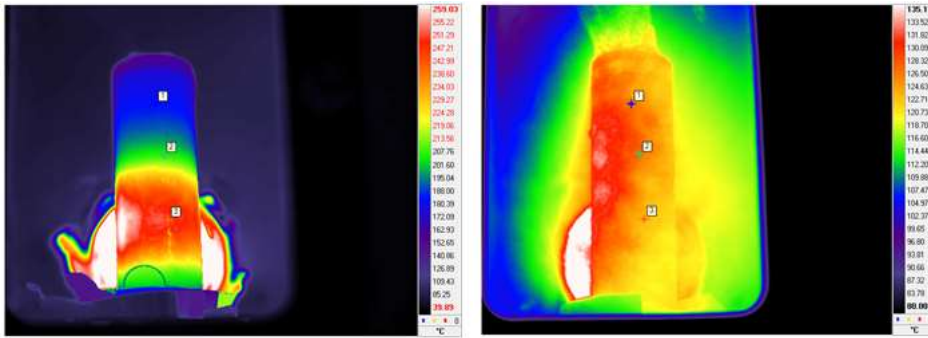


Fig. 71. Thermal image during the fast tomography thermal abuse experiments of $\text{Al}_{123} \text{FePO}_4$ batteries. Thermal image at point of explosion during the fast tomography thermal abuse experiments of $\text{Al}_{123} \text{FePO}_4$ batteries.

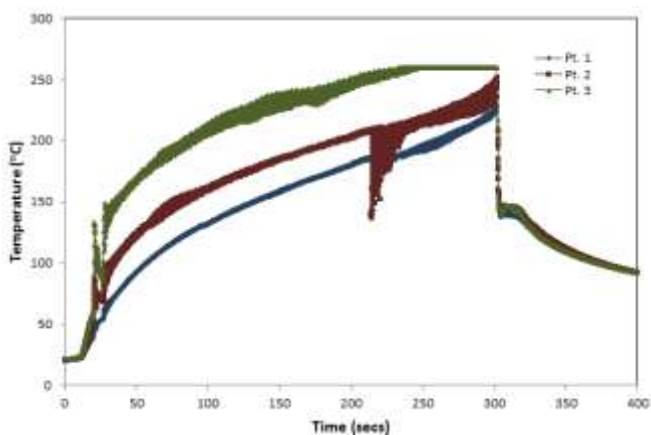


Fig. 72. Temperature plotted against time at points 1, 2 and 3 on the batteries surface. The drop in temperature at point 2 at around 200 s is due to electrolyte material flowing down the side of the battery after venting. After about 250 s the thermal cameras maximum temperature was reached; the maximum temperature reached by the battery was not captured.

Tomography:

Slow Tomography:

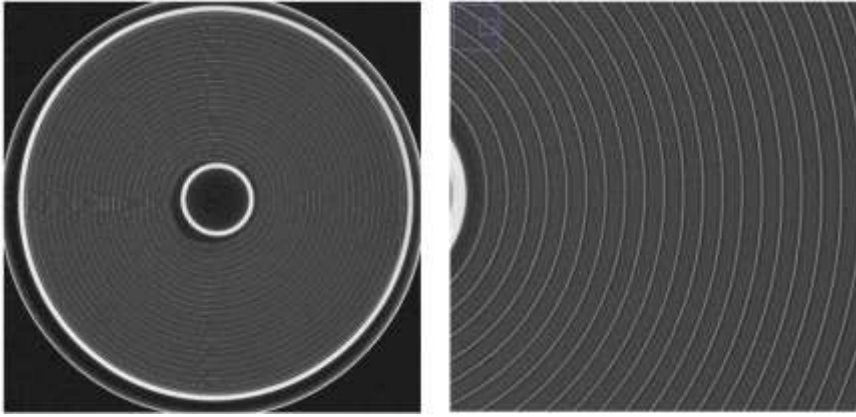


Fig. 73. Tomograph showing the initial state of the $A_{123} \text{FePO}_4$ battery before thermal abuse test. Tomograph focused on a region of the $A_{123} \text{FePO}_4$ battery for later comparison.

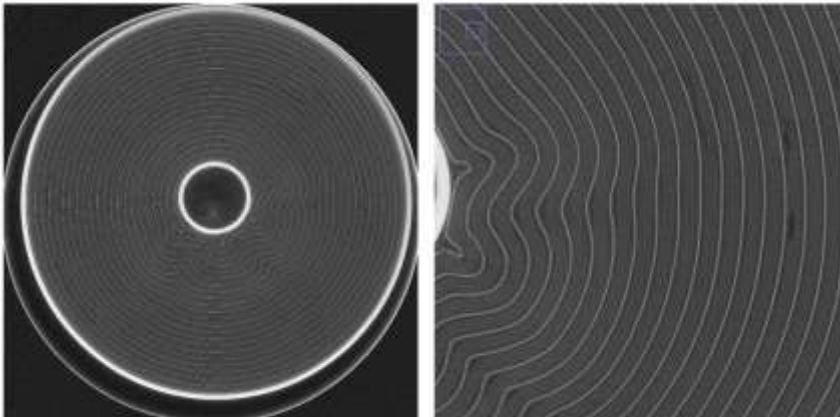


Fig. 74. Tomograph showing the state of the $A_{123} \text{FePO}_4$ battery during thermal abuse test. Tomograph focused on a region of the $A_{123} \text{FePO}_4$ battery showing evidence of structural deformation during thermal abuse test. Deformation believed to be induced from gas pocket formation.

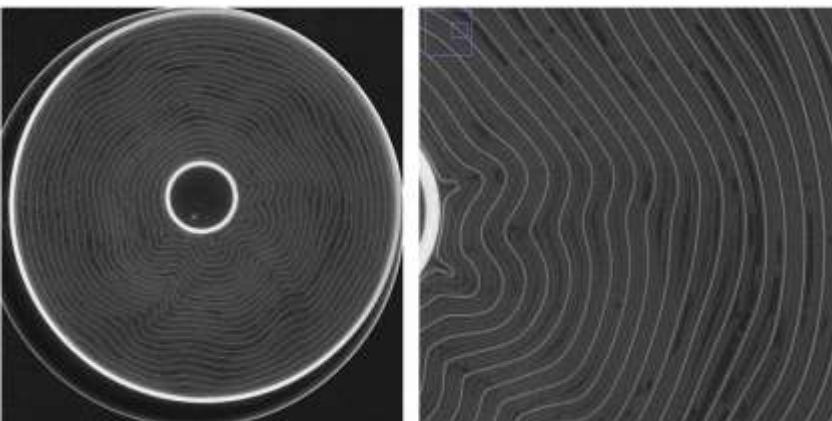


Fig. 75. Tomograph showing advanced stages of structural degradation of the $\text{Al}_{123} \text{FePO}_4$ battery during thermal abuse test, before complete thermal runaway. Tomograph showing advanced stages of structural degradation of the $\text{Al}_{123} \text{FePO}_4$ battery during thermal abuse test, before complete thermal runaway.

Fast Tomography:

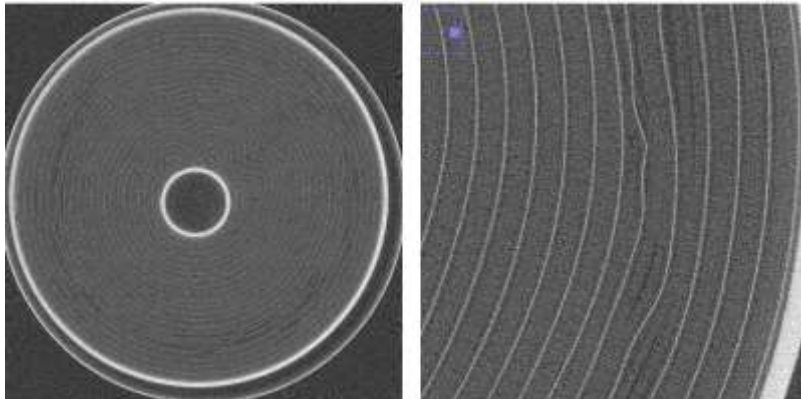


Fig. 76. Fast tomography tomograph showing the extent of degradation about 6 s before thermal runaway. Fast tomography tomograph showing evidence of delamination between the electrode and current collecting materials about 6 s before thermal runaway.

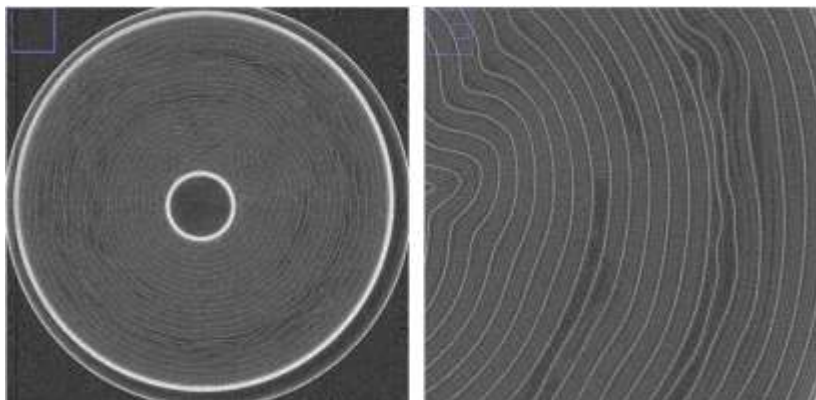


Fig. 77. Fast tomography tomograph showing the extent of degradation about 2 s before thermal runaway. Fast tomography tomograph showing the extent of degradation about 2 s before thermal runaway.

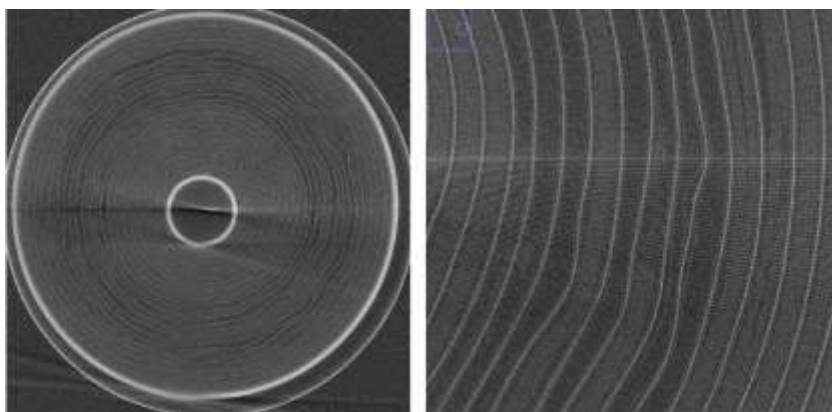


Fig. 78. Fast tomography tomograph capturing the state of the A123 FePO₄ battery at the point of initiation of thermal runaway. Image artefacts are caused by sample motion during the 0.4 second tomography scan. Fast tomography tomograph showing magnitude of degradation of the A123 FePO₄ battery at the point of initiation of thermal runaway. Image artefacts are caused by sample motion during the 0.4 second tomography scan.

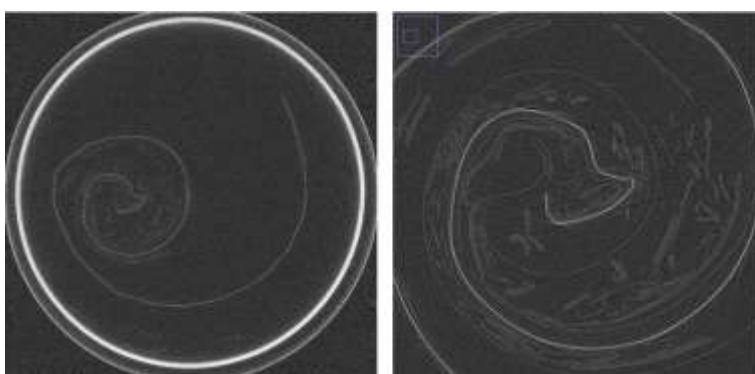


Fig. 79. Fast tomography tomography showing the remnants of the A123 FePO₄ battery after thermal runaway. Complete ejection of the battery internals occurred during thermal runaway. Fast tomography tomography showing the remnants of the A123 FePO₄ battery after thermal runaway. Complete ejection of the battery internals occurred during thermal runaway.



Fig. 80. Radiograph capturing the initiation of thermal runaway. A wavy electrode behavior is seen when scanning through the frames, believed to be caused by rapid gas generation and gas movement throughout the rolled material.



Fig. 81. Radiograph showing the moment before the ejection of the batteries internal materials.

Comments :

The A_{123} $FePO_4$ battery reached a much higher temperature (ca. 60 – 70 °C higher) than the NMC batteries before thermal runaway occurred. In addition, the presence of the internal cylindrical support appears to prevent the electrode collapse caused by the ‘*diapir*’ effect seen in the NMC cells. The A_{123} $FePO_4$ batteries appear to not only to have superior thermal stability but also superior structural support to the NMC cells, highlighting the importance of intelligent engineering.

The thermal runaway and ejection of contents appears to have occurred in < 0.05 s. A clear view of this process in the radiographs was hindered by the brightness of the beam after the contents were removed from view, Fig. 81. Both the aluminium and copper current collecting materials appear to be still intact after thermal runaway which when combined with the final temperature observed for the battery in Fig. 72, provide evidence that the battery and its internals did not reach as high of temperature during thermal runaway as the NMC cells.